Influence of rock fragment coverage on soil erosion and hydrological response: Laboratory flume experiments and modeling

S. Jomaa [a,*], D.A. Barry [a], B.C.P. Heng [b], A. Brovelli [a], G.C. Sander [c], J.-Y. Parlange [d]

[a] *Laboratoire de technologie écologique, Institut d'ingénierie de l'environnement, Faculté de l'environnement naturel, architectural et construit (ENAC), Station 2, Ecole polytechnique fédérale de Lausanne (EPFL), 1015 Lausanne, Switzerland*. Ph. +41 (21) 693-8073; +41 (21) 693-5576; +41 (21) 693-5919; Fax. +41 (21) 693-8035. E-mail addresses: seifeddine.jomaa@epfl.ch, andrew.barry@epfl.ch, alessandro.brovelli@epfl.ch

[b] *Building Research Institute, Housing and Development Board, Singapore.* Ph. +65 6490-3353; Fax. +65 6490-2662. E-mail address: peterheng@e.ntu.edu.sg

[c] *Department of Civil and Building Engineering, Loughborough University, Loughborough LE11 3TU United Kingdom*. Ph. +44 (1509) 223-777; Fax. +44 (1509) 223-981. E-mail address: g.sander@lboro.ac.uk

[d] *Department of Biological and Environmental Engineering, Cornell University, Ithaca, New York 14853-5701 USA*. Ph. +1 (607) 255-2476; Fax. +1 (607) 255-4080. E-mail address: jp58@cornell.edu

Accepted: *Water Resources Research,* 9 April 2012

*Author to whom all correspondence should be addressed

Abstract

Two laboratory flume experiments on the effect of surface rock fragments on precipitation-driven soil erosion yields were carried out. The total sediment concentration, the concentration of seven individual size classes and the flow discharge were measured. Digital terrain models (DTMs) were generated before and after one of the experiments. The results revealed that the rock fragments protected the soils from raindrop detachment and retarded the overland flow, therefore decreasing its sediment transport capacity. Rock fragments were found to affect selectively the different size classes in a manner that changed according to the time scale. For short times, the rock fragment coverage reduced erosion of the finer particles (< 20 μm). For the mid-size classes the protection decreased, while erosion of the larger size classes (> 100 μm) was unaffected. At long times the rock fragment cover decreased the concentration of the individual size classes in proportion to effective rainfall intensity and the area exposed to raindrops. An area-based modification of the Hairsine and Rose (H-R) soil erosion model was employed to analyze the experimental data. The H-R model predictions agreed well with the measured sediment concentrations when high rainfall intensity and low rock fragment cover were used. Predictions were instead less accurate with low rainfall intensity and high rock fragment cover. The DTM results showed that the presence of rock fragments on the soil surface led to increased soil compaction, perhaps due to higher soil moisture content (from greater infiltration) within the rock fragment-covered flumes.

Keywords: Hairsine-Rose model, Particle size distribution, Area-based soil erosion, Sediment concentration, Rainfall simulator, Soil compaction

1. Introduction

Surface rock fragments retard overland flow discharge, reduce the runoff generation rate as well as soil erosion and prevent the development of the surface sealing, which in turn increases the infiltration rate [*Poesen et al.*, 1990, 1994, 1998, 1999; *Abrahams and Parsons*, 1991, 1994; *Poesen and Lavee*, 1991, 1994; *Torri et al.*, 1994; *van Wesemael et al.*, 1995, 1996; *de Figueiredo and Poesen*, 1998; *Rieke-Zapp et al.*, 2007; *Smets et al.*, 2008; *Guo et al.*, 2010]. In Mediterranean areas where soils rich in rock fragments represent more than 60% of land, rock fragments on the soil surface reduce soil erosion by intercepting raindrop splash and impeding flow-driven entrainment processes [*Poesen and Lavee*, 1994]. Additionally, they reduce the cross-sectional flow area and rill development, resulting in increased flow path meandering and higher overland flow depths. During the early stage of a rainfall event, this increased overland flow depth leads to increased infiltration into protected areas around and under the rock fragments [*Adams*, 1966; *Koon et al.*, 1970; *Poesen and Ingelmo-Sanchez*, 1992; *Bunte and Poesen*, 1994; *Cerdà*, 2001; *Jomaa et al.,* 2012].

Using different rock fragment coverages, *Jomaa et al.* [2012] showed that, under controlled laboratory flume conditions (similarly sized rock fragments and hand cultivated and smoothed soils), precipitation-driven soil erosion is proportional to the area of soil exposed and the effective rainfall. In addition, they showed that the proportionality is controlled to a small extent by the soil's initial conditions (such as initial moisture content and surface characteristics). In other words, when the initial conditions are more complex, the area-based approach is obtained only at steady state. On the other hand, using field data, it was found that rain splash is in general not proportional to the area exposed [*Jomaa et al.,* 2012]. However, other studies found that the effect of rock fragments on soil erosion is more complex and ambivalent (could be positive or negative) depending on the features of the rock fragments (fraction of soil surface covered, rock fragment size and shape and emplacement –

resting on the soil surface, partially or totally embedded in the soil matrix) [*De Ploey,* 1981; *Poesen and Ingelmo-Sanchez,* 1992; *Loosvelt*, 2007; *Jomaa et al.,* 2012] and overland flow characteristics (flow velocity, water depth, shear velocity) [e.g., *Boyer and Roy*, 1991; *Bunte and Poesen,* 1993; *Papanicolaou et al.,* 2011].

The coupling between overland flow and surface rock fragments has been studied intensively in particular in situations where flow-driven entrainment is the dominant sediment transport mechanism. Numerous studies have indicated that a key parameter controlling the flow characteristics around obstacles (i.e., for example rock fragments) is the ratio of the flow depth, D, to the diameter of the rock fragment, d_r, which is defined as "relative depth or submergence" [e.g., *Dermisis and Papanicolaou,* 2010; *Papanicolaou et al.,* 2011]. Most of these studies have focused solely on examining the erosion and flow patterns around rock fragments for high relative submergence conditions, limited studies, however, were conducted under low relative submergence [*Papanicolaou and Kramer,* 2005; *Yager et al.,* 2007]. The effect of surface rock fragments when rain splash is the dominant erosion mechanism has been little investigated. A summary of the literature on the effect of rock fragments on soil erosion and associated hydrological response is given in Table 1.

Table 1 near here

Numerous studies have pointed out the desirability of incorporating within process-based models the effect of surface rock fragments on soil erosion production and hydrological processes. For instance, *Poesen et al.* [1999] found that the rock fragment cover (R_c) reduced soil erosion yield (E) exponentially, i.e., $E = \exp(-bR_c)$, where b is an empirical coefficient that depends on the initial moisture content, the scour hole that develops around the rock fragments and the bed armoring. Additionally, they highlighted that the rock fragments provide greater protection to initially wet soils than to initially air-dry soils (i.e., b varies according the initial state of the topsoil).

de Figueiredo and Poesen [1998] highlighted that few soil erosion models take account of surface rock fragment effects. Rock fragments (i) increase hydraulic roughness and friction, decreasing the overland flow speed and sediment yield, as found in the WEPP model [*Nearing et al.,* 1989], for example; and (ii) reduce the cross-sectional flow area leading to reticular flow in the vicinity of rock fragments and increasing the local erosional capacity [*Bunte and Poesen*, 1993]. The EUROSEM erosion model [*Morgan et al.,* 1990, 1998] considers the effect of rock fragment cover and position on the effective infiltration rate and saturated hydraulic conductivity, which in turn affect soil erosion delivery. Within EUROSEM, rock fragments resting on the topsoil provide protection to the surface soil structure and promote infiltration, however when they are embedded in the soil matrix they reduce infiltration [*Veihe et al.,* 2000]. The KINEROS model [*Woolhiser et al.*, 1990] accounts for rock fragments by considering the fraction of the surface soil occupied by rock fragments, which in turn affects the infiltration rate. Both these effects are likely more important for shear- rather than precipitation-driven erosion. However, the effect of rock fragments in increasing the overland flow depth (relative to the case of no rock fragments) will affect precipitation-driven erosion due to attenuation of the raindrop impact on the soil surface.

Although the effect of surface rock fragments on the cumulative sediment delivery has been investigated, there have been no studies on the effects of surface rock fragments on individual sediment size classes, including the extent to which erosion of the different size classes in rock fragment-protected soils is controlled by rainfall characteristics and the initial soil moisture content. *Mandal et al.* [2005] and *Martinez-Zavala and Jordan* [2008] reported – using pre-eroded, natural field soil – that the silt was the dominant fraction (more than 50%) of the total eroded mass at the flume exit due to the reduction of the sealed surface (area protected by the rock fragments). While silt moved with the overland flow, the clay and sand fractions remained on the soil surface and formed

the surface seal (clays) and the deposited layer (sand) [*Mandal et al.,* 2005; *Martinez-Zavala and Jordan* 2008]. In the following, erosion of individual size classes is considered using the 1D Hairsine-Rose (H-R) model [*Hairsine and Rose*, 1991]. This model simulates size class-dependent erosion and deposition processes, and predicts the development of a shield layer composed of (re-)deposited sediment, which acts to protect the original soil. Below, this sediment is referred to as the deposited layer. The H-R model, which developed the earlier model of *Rose et al.* [1983a, 1983b], has been investigated and validated in numerous studies for simple scenarios and with appropriate assumptions [e.g., *Rose et al.*, 1994, 2007; *Sander et al.*, 1996, 2007, 2011; *Hogarth et al.*, 2004; *Barry et al.*, 2010; *Jomaa et al.*, 2010; *Heng et al*., 2011]. However, the H-R model has not been used for the situation where the soil is covered partially by rock fragments. It is therefore appropriate to test the model for this case.

The aims of this study were (i) to quantify how the rock fragment coverage affects the total sediment concentration and the concentrations of the individual size classes, (ii) to test if rock fragment cover affects preferentially a particular size class within the eroded sediment and (iii) to determine whether the 1D H-R erosion model can represent the experimental data.

2. Methods

2.1. Experimental setup and experiments (H6 and H7-E1)

Two laboratory experiments under simulated rainfall of 74 and 28 mm h^{-1} (measured using a pluviometer), denoted H6 and H7-E1, respectively, were carried out using the EPFL erosion flume [*Viani*, 1986; *Baril*, 1991]. The rainfall intensities used in this study (28 and 74 mm h^{-1}) are realistic rainfall intensities for Lausanne city (Switzerland, [*Baril*, 1991]) and, more generally, for central Europe. The lower rainfall rate is a little above 25 mm h^{-1}, the value reported as a threshold for

significant erosion [*Morgan*, 2005]. The higher value is representative of the maximum intensity expected for Lausanne.

Spatially near-uniform precipitation was applied to the soil (uniformity coefficient of 0.86, *van-Tromp Meerveld et al.* [2008], *Jomaa et al.* [2010]). In order to characterize the temporal distribution of the simulated raindrops, the raindrop size distribution (DSD) technique can be used [e.g., *Elhakeem and Papanicolaou,* 2009]. The temporal variability of raindrops were characterized using a Parsivel Disdrometer (manufactured by OTT, http://www.ott.com, last accessed 26 December 2011). Results showed that the rainfall simulator provides a nearly constant DSD during each precipitation event, with an average drop size of 2.2 mm. The simulated DSD compares well with the natural rainfall measured by a network of disdrometers on the EPFL campus [*Jaffrain et al.,* 2011].

The 6-m × 2-m EPFL rainfall simulator – here divided into two identical 6-m × 1-m flumes – has been described in detail elsewhere [*Tromp-van Meerveld et al.*, 2008; *Jomaa et al.*, 2010, 2012]. The flumes were filled with 0.32 m of a loam agricultural soil (4% of clay, 29% of silt, 41% of sand and the rest is fine gravel) from a field near Sullens (Vaud), Switzerland. Under the FAO classification [*IUSS Working Group WRB*, 2007], the soil is a cambisol, which is very common in Switzerland. Details of the soil's characteristics were given by *Baril* [1991]. On the bottom of flumes, 0.10 m of coarse gravel facilitated drainage. The soil surface was prepared in order to ensure consistent initial conditions (roughness). Before the experiment, the top 0.2 m of the soil surface was hand cultivated and gravel (> 2 cm) removed. Then the soil surface was smoothed using a mechanical system that ensured a uniform, smooth surface. Before the experiments, the soil was hand cultivated to create a smooth surface and precipitation was applied immediately. Similar initial bulk densities were ensured for both experiments (1.11 and 1.14 g cm^{-3} for H6 and H7-E1, respectively).

Experiments were conducted with a fixed slope of 2.2%. In flume 1, bare soil was used, while flume 2 had 20 and 40% rock fragment coverage for experiments H6 and H7-E1, respectively (Figure

1). Irregularly shaped natural rock fragments (diameters in the range 5-7 cm) were placed on the surface (not embedded in the soil matrix). Rock fragments were arranged in rows transverse to the slope (Figure 1), forming a regular triangular pattern. In addition, the topsoil surface used in both experiments had a relatively similar and low initial water moisture content measured to be 6.81 and 8.84% for H6 and H7-E1, respectively.

Stream power calculations were used to ascertain whether entrainment in the overland flow contributed to soil erosion [*Beuselinck et al.,* 1999; *Kinnell*, 2005]. According to *Beuselinck et al.* [2002], for loamy soils the critical stream power above which entrainment occurs is in the range 0.15-0.20 W m^{-2}. Among the experiments considered in this work, H6 with bare soil had the highest runoff rate (Table 2) and therefore the largest stream power. Based on the calculations reported by *Jomaa et al.* [2010], the estimated stream power for H6 was around 0.02 W m^{-2}, much lower than the threshold (0.15 W m^{-2}). This indicates that rain splash was the dominant erosive mechanism in all flume experiments, while the contributions of overland flow and rill erosion were less significant.

Experiments H6 and H7-E1 had a duration of 3 and 2 h, respectively. During this time, effluent was collected at the flume exits for later analysis. Details of the experiments are given by *Jomaa et al*. [2010], who provide the characteristics of each rainfall event and the topsoil surface properties, rock fragment features as well as the measured hydrological response of each experiment. To indicate how rock fragments control locally the soil erosion and flow hydraulics, light-colored plastic particles were spread uniformly in a transverse band across flume 2 at 1.5 m (Figure 2). The particles had a density close to that of water (960 kg m^{-3}), and were approximately spherical with a diameter of about 2.5 mm, which is roughly a quarter of the mean steady state overland flow depth. These characteristics ensure that they move easily with the overland flow and become trapped in shallow areas and around the rock fragments.

Figure 1 near here

During experiment H6, the volumetric moisture water content was measured within the flume soil for up to 12 h at different depths using ten 5TE probes (Decagon, Inc. Pullman, USA, http://www.decagon.com, last accessed 5 August 2011). Three probes were embedded in the middle of each flume – 1.8 m from the upstream start of the flume (Figure 1) – at three different depths (5, 10 and 20 cm). Two probes were embedded in two soil profiles (10 and 20 cm deep) at 2.5 m, which is one the four transversal lines characterized by increased raindrop compaction due to the sprinklers overlapping (Figure 2).

In order to describe the flow regime, the Froude number (*Fr*) for the steady-state overland flow is reported in Table 2 for the two experiments. The total sediment concentration and the individual size class concentrations were measured as well as the discharge rate over the course of the each experiment.

Table 2 near here

2.2. Digital terrain models (DTM)

DTM's of the soil surface before and after experiment H6 (Figure 2) were generated as a means of assessing (i) the soil surface uniformity before the experiment began and (ii) the differences between the flumes at the experiment's conclusion. Scans were performed using a FARO Laser Scanner (http://www.faro.com, last accessed 4 August 2011). Scanner characteristics and details of the DTM were described by *Jomaa et al.* [2010]. The scanner used had vertical and horizontal angular resolutions of 9×10^{-3} and 7.6×10^{-4} degrees, which resulted in a theoretical spatial resolution of less than a millimeter.

Figure 2 near here

2.3. Modeling

2.3.1. Governing equations

The H-R model was adapted to account for the shielding effect of rock fragments, i.e., the rock fragments reduce the cross-sectional area and provide additional protection to the original soil base. The governing equations of H-R erosion model have been described in detail previously [e.g., *Sander et al.*, 1996; *Lisle et al.*, 1998; *Parlange et al.*, 1999; *Sander et al.*, 2007; *Tromp-van Meerveld et al.*, 2008; *Heng et al.,* 2009]. Here, a brief summary of the H-R model taking into account the effect of the rock fragment cover is presented. *Jomaa et al.* [2012] found that, in controlled laboratory conditions, precipitation-driven soil erosion is proportional to the area exposed and the effective precipitation. Thus, the H-R model equations were adjusted based on the area not covered by rock fragments:

$$\eta \frac{\partial D}{\partial t} + \frac{\partial q}{\partial x} = R, \tag{1}$$

$$\eta \frac{\partial (Dc_i)}{\partial t} + \frac{\partial (qc_i)}{\partial x} = \eta (e_i + e_{ri} - d_i), \tag{2}$$

and

$$\frac{\partial m_i}{\partial t} = d_i - e_{ri}, \tag{3}$$

where t is time, x is downslope distance, D is overland flow depth, c_i is the suspended sediment concentration, m_i is the deposited sediment mass per unit area for the size class i (seven size classes were used: < 2, 2-20, 20-50, 50-100, 100-315, 315-1000 and > 1000 μm), q is the volumetric water flux per unit width, R is the steady-state excess rainfall rate, and η is the average proportion of the cross sectional area not covered by rock fragments. Note that (1) assumes that the height of the water surface is below the height of the rock fragments. The source/sink terms e_i, e_{ri} and d_i are, respectively,

the detachment and re-detachment rates due to rainfall and the rate of deposition with units of mass per unit area per unit time. The rates of rainfall detachment from the original soil and from the deposited layer are, respectively:

$$e_i = (1 - H)\, p_i a P \tag{4}$$

and

$$e_{ri} = H \frac{m_i}{m_t} a_d P, \tag{5}$$

where a is the detachability of the original soil, a_d is the detachability of the re-deposited soil in mass per unit area per unit flow depth, p_i is the proportion of class i sediment in the original soil, which was measured for the seven size classes from the grain size distribution of the original soil, $m_t = \sum m_i$ is the total deposited sediment mass per unit area, $H = \min(m_t / m_t^*, 1)$ represents the degree of shielding of the original soil provided by deposited sediment, and m_t^* is the mass of deposited sediment required to shield the original soil completely. The rate of deposition for sediment class i is given by $d_i = (v_i + f)\, c_i$, where v_i is the settling velocity of particles in that class and f is the infiltration rate.

Sander et al. [1996] presented an approximate analytical solution to the above model that agreed well with experimental data obtained from different rainfall flumes with appropriate assumptions [*Proffitt et al.*, 1991; *Tromp-van Meerveld et al.,* 2008; *Jomaa et al.*, 2010]. Following (1) and (2), their solution was adjusted to account for the shielding effect of the rock fragment cover and used in the data analysis below.

2.3.2. Model assumptions

Assumptions of the H-R theory with large influence on model predictions and parameter estimation can be summarized as follows:

- Rainfall-induced erosion is affected by the water depth over the soil. Typically, the erodability of the soil declines exponentially with water depth, with a characteristic length scale of a few raindrop diameters [*Moss and Green*, 1983; *Proffitt et al.*, 1991].
- After erosion, it is assumed by the H-R model that the particles enter the overland flow as suspended load, and settle back to the soil bed at the same rate of settling as a single particle in a quiescent fluid. This simplified picture ignores other mechanisms that can influence soil erosion, such as: (i) the impulsive movement of particles due to direct impact by raindrops; (ii) soil morphological variations leading to variable depths of water over the surface; (iii) hindered settling due to high sediment concentrations; and (iv) bedload sediment transport. For very shallow depths and relatively large particles, it is apparent that these factors could markedly affect soil erosion, e.g., the concept of suspended load for grain sizes of about 1 mm would be questionable for a flow depth of a couple of millimeters.
- The material settling back to the soil bed forms the protective deposited layer. Prediction of this layer is a key attribute of physically based soil-erosion models, including the H-R model used here.
- The approximation of *Sander et al.* [1996] assumes that spatial variations are negligible compared with temporal variations, i.e., they dropped the spatial derivative terms in the model presented above. The validity of this assumption depends on the boundary and initial conditions for which the kinematic and sediment mass conservation equations are solved. Whether this approximation holds depends on the experimental conditions and it cannot be assumed in general. For the experiments with bare soil presented in this work (rain-splash driven, without water inflow), it is equivalent to assume that the soil surface is homogeneous, i.e. detachment/deposition are spatially uniform or that the characteristic length scale of heterogeneity is much smaller than the plot size.

Since the soil surface was leveled and smoothed before the experiment, the assumption appears reasonable. *Sander et al.* [1996] and *Tromp-van Meerveld et al.* [2008] discussed this simplification and showed that it is reasonable for data collected from experiments with a gentle slope, under homogenous rainfall and from regular topography. Additionally, *Hogarth et al.* [2004] showed that during a rainfall-driven erosion event, the sediment concentration has a strong variation with time; however, its spatial variation appears very small except at very short times.

2.3.3. Model application and parameter estimation

The H-R model assumes that raindrop detachment is not particle-size selective [*Rose* 1960, 1962]. However, during sediment transport the model predicts particle size class sorting due to the differing settling velocities [*Hairsine and Rose*, 1991]. The finer particles settle out of the water column more slowly than the coarser materials and hence are transported further by the overland flow. As mentioned above, the sediment concentration data were divided into seven size classes, and for each a single settling velocity was assigned. The settling velocities of all size classes were taken from *Tromp-van Meerveld et al.* [2008] who used the same experimental facility and soil. They noted that there could be several factors affecting settling velocities such as surface water depth, infiltration rate, measurement errors, particle shape, etc. These factors lead to the conclusion that, for modeling purposes, it is appropriate, for a given range of particle sizes, to permit a corresponding range of settling velocities [*Tromp-van Meerveld et al.*, 2008], with the choice within that range depending on the quality of the model's predictions. The range of the settling velocities for each size class and the values used are reported in Table 3. In order to fit the model to the experimental data, three other parameters, a, a_d, and m_t^* were adjusted also. Following *Jomaa et al.* [2010], first, these parameters were adjusted manually until reasonable fits with the data were obtained. Second, an automated parameter estimation procedure was implemented to perform a better calibration.

Table 3 near here

3. Results

3.1. Laboratory flume experiments

3.1.1. Experiment H6

The time-to-runoff (time between the beginning of rainfall and the start of first outflow at the flume exit) for flumes 1 and 2 were, respectively, 6.07 and 8.28 min. The presence of rock fragments on the surface of flume 2 increases the time-to-runoff (Table 3, *Jomaa et al.* [2012]). In addition, the results revealed that the flumes had different total overland flow fluxes (Figure 3), and that the steady-state discharge rates were achieved at different times for each flume and during each experiment (Table 2). Steady-state excess rainfall rates R were obtained as average values during these steady-state periods. Using the kinematic approximation for the steady-state discharge of the both flumes, $q = Rl$ (l = 6 m is the length of the flume), R was estimated for flumes 1 and 2 as 68.7 and 54.4 mm h^{-1}, respectively (Table 3, *Jomaa et al.* [2012]).

Figure 3 near here

The infiltration rate (f) was calculated as the difference between the rainfall intensity (P) and the steady-state excess rainfall rate (R):

$$f = P - R. \tag{7}$$

Using (7), the infiltration rates, f, determined for flumes 1 and 2 were 5.3 and 19.6 mm h^{-1}, respectively. The presence of rock fragments on flume 2's topsoil increased slightly the time-to-runoff (Figure 3) and considerably the infiltration rate. The rock fragment layout on the soil surface not only reduced the cross-sectional area available for flow but also increased the possibility of flow path meandering. Additionally, the rock fragments protected the soil against raindrop impact-induced

surface sealing and permitted higher infiltration rates in zones around and under the rock fragments, increasing the time-to-runoff relative to the case of no surface rock fragments. In unprotected areas, surface compaction/sealing during precipitation reduces the infiltration rate significantly [*Moore and Singer*, 1990; *Le Bissonnais et al.,* 1995; *Assouline*, 2004].

The total and the individual size classes' sediment concentrations of flumes 1 and 2 showed consistent behavior (Figure 4) for experiment H6, with a short time peak occurring at the beginning of the erosion event for all size classes. That is, all size classes contribute to the early short time peak in the total sediment concentration. Initially, all particle motion is due wholly to raindrop splash, which affects all class sizes without evident discrimination [*Rose*, 1960, 1962]. As surface flow initiates, raindrop impact is attenuated negligibly and thus sediment concentrations in the overland flow are maximized, leading to high sediment concentrations in the flume runoff. This behavior is consistent with the data presented by *Jomaa et al.* [2010].

Comparing the total sediment concentrations collected from flumes 1 and 2 (without and with rock fragments, respectively) during experiment H6, the results show that the rock fragments reduced slightly the total mass eroded. The reduction is proportional largely to the area exposed and the effective rainfall, although the initial moisture content and bulk density play a small role [*Jomaa et al.*, 2012]. However, the sediment size class concentrations show different behavior. Here, the rock fragments have a selective effect that varies with time scale. For long times, the sediment concentrations were reduced for all size classes proportionally to the area exposed to raindrops and effective rainfall. This effect was slightly more pronounced for the finer size classes (< 2 and 2-20 μm). At early times, the results showed that the rock fragments have a more selective effect depending on the individual size classes. The main short-time signal is the peak in sediment concentration, for which the rock fragments decreased significantly the sediment concentration of the

two finest size classes (< 2 and 2-20 μm). For the mid-size classes (20-50 and 50-100 μm), as the particle size increased, the protection decreased in comparison to the two finest classes (Figure 4). However, the rock fragment cover increased the short-time peak of the larger size classes (100-315 and 315-1000 μm). For the largest class (> 1000 μm), the data show considerable scatter although they appear to be consistent with the rock fragments having no effect.

Figure 4 near here

The moisture content measurements showed that in the non-overlapping region the moisture content at 5 cm was greater than at locations deeper in the profile (Figure 5). For the most part, the moisture content in flume 2 (20% coverage) responded more rapidly than in flume 1 (no rock fragments), reflecting the greater overland flow depth on flume 2. However, the probe located at the depth of 5 cm in flume 1 responded earlier than the corresponding probe in flume 2. This likely results from the greater initial moisture content in flume 1 (8.81% in flume 1, 6.42% in flume 2). Additionally, the rock fragments increased the long-time (steady-state) moisture content (Figure 5). Note that the water infiltrated beyond the 20-cm depth in flume 2 due to the unsealed areas in vicinity of rock fragments, whereas the moisture content did not change at this depth in flume 1.

Figure 5 near here

3.1.2. Experiment H7-E1

Even though initially the soil was slightly wetter for experiment H7-E1 than for H6, the time-to-runoff from flume 1 was 8.25 min longer than was observed for experiment H6 for the same flume (6.07 min), reflecting the different precipitation rates used in each experiment. The results showed that the time-to-runoff was longer for flume 2 (with rock fragments, 27.13 min). The steady-state infiltration rate for flume 1 was about 7.54 mm h^{-1} (estimated based on the runoff rate during the final

10 min of the experiment). However, the 40% rock fragment cover on flume 2 increased the steady infiltration rate to about 13.4 mm h^{-1}. The measured total sediment concentration collected from flume 1 during experiment H7-E1 (Figure 6) is considerably lower than that from the same flume during experiment H6 (Figure 4), supporting the notion – included in the H-R model in (4) and (5) – that the interrill soil erosion is proportional to rainfall intensity. The measured sediment concentration from flumes 1 and 2 during experiment H7-E1 showed a consistent short time peak for all size classes, except perhaps for the largest size class where the data show considerable scatter. In contrast to experiment H6, at the beginning of experiment H7-E1 the concentrations of the individual size classes increased gradually until reaching a peak, and then decreased gently to the steady-state concentrations, while the sediment concentrations decreased rapidly during H6. Also, the results suggest that fully steady-state behavior was not reached during experiment H7-E1 especially for bare-soil conditions, probably due to the low precipitation rate compared with experiment H6 (28 and 74 mm h^{-1}, respectively). The sediment concentrations of the individual size classes became relatively constant for experiment H6 after about 1.5 h after runoff commenced. However, for experiment H7-E1, the steady-state equilibrium was not reached during the 2-h rainfall event. Therefore, the results also showed that the presence of rock fragments on the topsoil surface reduced the time needed to reach steady state compared with bare soil (Figure 6). This reflects the reduction in rain splash erosion caused by rapid development of the overland flow depth (which results from the reduction of the flow cross-sectional area by rock fragments). This was less pronounced in experiment H6, probably due to the high rainfall intensity and to the low rock fragment coverage compared with H7-E1.

The results collected from experiment H7-E1 showed that the rock fragments reduced the sediment concentration of the two finest sizes (< 2 and 2-20 μm). The same effect was even more

noticeable for the mid-sizes (20-50 and 50-100 μm) (Figure 6). This reduction was maintained for the duration of the experiment. For the larger particles (up to 100 μm), the presence of rock fragments on the topsoil reduces sediment delivery at steady state whereas at short times rock fragments do not provide any protection for the large size classes (Figure 6). Even though there is considerable scatter for the largest size class (> 1000 μm), it is clear that rock fragments reduce the contribution of these particles as well. This reduction in effluent sediment concentrations was greater for H7-E1 (for all size classes) than for H6, due to the effect of the greater rock fragment coverage for H7-E1.The results from experiment H7-E1 are consistent with those of experiment H6 and highlight that the rock fragments affected selectively the different particle size classes in the soil. During the initial phase of the erosion event (short-time behavior), rock fragments reduced considerably the delivery of the finer size classes, while they did not provide protection for the medium and large size classes. At steady state, the presence of rock fragments on the topsoil surface reduced the concentrations of all size classes proportionally to the effective rainfall and area exposed to raindrop detachment [*Jomaa et al.*, 2012].

Figure 6 near here

3.1.3. The umbrella effect

"Umbrella" refers to the protection against raindrop detachment afforded by the rock fragments above the soil surface. It was found that the colored plastic particles added at the upstream of flume 2, as shown in Figure 2, became trapped on the downstream side of the rock fragments (Figure 7). In addition to the colored particles, visual observations after the experiments showed that rock fragments protect the underlying original soil against raindrop detachment and surface sealing. The protected soil does not undergo compaction, and thus allows locally increased infiltration. Previous experiments [*Boyer and Roy*, 1991] demonstrated that the downstream sides of rock fragments act as particle

trapping zones. Particles can also be transported into this zone by raindrop splash and, once there, the umbrella effects stops raindrops splashing them back out again.

Figure 7 near here

3.1.4. Hydraulics and DTM maps

The *Fr* values (range of 0.03-0.07, Table 2) were smaller than the critical value (about 1), i.e., all experiments had sub-critical flow regimes [*Grant,* 1997; *Rieke-Zapp et al.,* 2007]. This is consistent with the stream power calculation, and further indicates that flow-driven soil erosion had a negligible contribution in all experiments (and therefore rain splash detachment was the dominant soil erosion process).

The DTM maps further indicate that sediment transport is not entirely 1D (Figure 2). In flume 1 (no rock fragments), after the experiment the micro-topography was not homogenous. The DTM results in Figure 2 suggest some meandering preferential flow paths, albeit of limited size, that were almost invisible when looking visually at the soil surface. On the contrary, in flume 2 (with rock fragments) the bed morphology was more homogenous indicating that the presence of rock fragments on the topsoil reduced the opportunity for preferential paths to form. Additionally, the DTM revealed that the presence of rock fragments on the topsoil surface increased surface compaction. Cross sections of the DTM along the transects depicted in Figure 1 are reported in Figure 8. The top panel (Figure 8a) shows the topsoil elevation in an area receiving rainfall from a single sprinkler. The elevation of the two flumes is shown on the same plot. The change in soil elevation (and thus compaction) is significantly more marked in the flume with rock fragments, with an average value of about 6-8 and 8-12 mm in flumes 1 and 2, respectively. The bottom panel (Figure 8b) instead shows the area characterized by overlapping sprinklers. In these areas, a similar elevation decrease was observed in the two flumes, on average in the range 1-1.2 cm, with a maximum change of 1.5 cm.

Figure 8 near here

4.1. Modeling

4.1.1. Experiment H6

The analytical solution of *Sander et al.* [1996] was used to fit the experimental results from flume 1. The fitting procedure followed that of *Jomaa et al.* [2010]. Three parameters, a, a_d and m_t^*, were optimized based on the measured and fitted sediment concentrations. Parameters were constrained within ranges based on their physical meaning and previous experiments using the same soil and flume. In particular, the fitting was performed using similar optimized values and the same particle settling velocities as *Jomaa et al.* [2010]. The model prediction for experiment H6 is shown in Figure 4. During the fitting, priority was given to adjusting the model to reproduce the experimental data of the finer size classes (> 2 and 2-20 μm). Following *Jomaa et al.* [2010], the overland flow depth, D, was fixed at 9 mm. The time-to-runoff was about 0.1 h. Recall that, during this period, raindrops land directly on the soil surface unattenuated by the overland flow layer, resulting in high sediment concentrations at the start of runoff. The initial measured effluent concentration values were used in the model as the initial sediment concentrations for each size class. At long times, the sediment distribution in the effluent should match that of the original soil [*Proffitt et al*., 1991], behavior that is reproduced by the H-R model. However, the particle size fraction of the original soil was not that of the steady-state effluent concentrations. A possible reason of this is aggregate breakdown [*Legout et al.*, 2005], which is not accounted for in the H-R model. Thus, in applying the H-R model, the size classes' proportions were adjusted to match the measured data. The fitting of the *Sander et al.* [1996] analytical solution yielded the parameter values reported in Table 2, together with the thickness of the shield layer approximated using (7) of *Jomaa et al.* [2010]. Correlation coefficients (r^2) were

determined separately for the three finest sediment classes (> 2, 2-20 and 20-50 μm), and for the rest of the particles, except the largest size class, which displayed significant scatter (Table 2).

The model reproduces quite well all the individual size classes except the largest (> 1000 μm) (Figure 4). This occurs since the larger particles move more via saltation or rolling than as suspended in the overland flow as assumed in the H-R model [*Sander et al.*, 1996; *Asadi et al.*, 2007]. The model could not predict the early peak sediment concentrations of this size class generating a slight short-time underestimation of the total sediment concentration. On the other hand, it was found that the measured settling velocities of the fine and the mid-size classes (< 2, 2-20, 20-50 and 50-100 μm) resulted in reasonable model predictions. The settling velocities of the larger size classes (100-315, 315-1000 and > 1000 μm), as with *Tromp-van Meerveld et al.* [2008] and *Jomaa et al.* [2010], were reduced to obtain reasonable model predictions. In shallow water, the high sediment concentrations generated by the raindrop impact affect the settling velocities and may inhibit the particles from reaching their final settling velocities. Particularly at the initial stage of the erosion event, the larger particles (about 1-2 mm) are influenced by this as their size is of the same order of magnitude of the overland flow [*Tromp-van Meerveld et al.*, 2008].

Model results are sensitive to the mass of soil per unit area needed to complete the shield layer, m_t^*. From this value (fitted in the model), we determined the thickness of the shield layer, z, as about 0.067 mm. Of course, this is an average value, whereas over the flume considerable variability would occur. The estimated value of the shield layer thickness is non-physical since it has the same order of magnitude as the grain size. The H-R model assumes that a homogenous shield layer develops over the entire eroded zone, which is unlikely due to the irregular topography and the sprinklers overlapping (Figure 2). The calibrated value is therefore interpreted as an average over the entire surface, and reflects this variability.

The H-R model (§2.3.1) was used to fit the sediment breakthrough curves of flume 2 (20% rock fragment cover). Relative to the bare soil, the presence of rock fragments affects the development of overland flow. At the commencement of rainfall and before overland flow develops, the rock fragments prevent surface sealing beneath them, maintaining a higher infiltration rate. During this initial stage, overland flow occurs later and is shallower. After the surface soil becomes saturated, the overland flow depth increases due to the reduced cross sectional area. The approximate solution of *Sander et al.* [1996] to the H-R model uses an average overland flow depth, D, which was determined from the long-time behavior. The overland flow depth was variable (since the soil surface was not smooth), but from measurements an average of about 11 mm was determined. Using this value and the flume 1 parameters, the modified H-R model was able to reproduce the flume 2 sediment concentration data (Figure 4), at least in a manner consistent with modeled flume 1 data. However, when the value of a (detachability coefficient of the parent soil) was slightly reduced compared with that used in flume 1 (7 instead of 10 mg cm^{-3}), the fitting of the experimental data improved. This is due to the increase in the overland flow depth in flume 2 from the rock fragments, and is consistent with the relationship between detachability and flow depth given by *Proffitt et al.* [1991] (detachability decreases with increased flow depth). After imposing the initial concentrations, the model reproduced the early selective effect of rock fragments on the various size classes.

4.1.2. Experiment H7-E1

The data collected from flume 1 during the experiment H7-E1 were fitted using the same procedure described above for experiment H6. The model initial conditions were adjusted according to the experimental setup (rainfall intensity, steady-state infiltration, overland flow depth and initial measured sediment concentrations). As explained above, the size class proportions used in the model were determined from the measured sediment concentrations in the effluent during the final 10 min of

the experiment – even though the steady state had not been truly reached for all sediment sizes. The low rainfall intensity (28 mm h^{-1}) used in this experiment generated a very shallow overland flow depth of about 2-4 mm. In the fitting procedure, the overland flow depth was fixed at 3 mm.

The H-R model unable to predict well all the individual size classes using the same parameters as used in experiment H6 (Figure 6). *Proffitt et al.* [1991] and *Misra and Rose* [1995] showed experimentally that the parameters quantifying the detachment of the original and deposited soil (a and a_d) vary with soil crusting as well as the overland flow depth, which differs between the experiments. They reported that, as D increases, the rainfall detachability of both the original soil and deposited layer should decrease, which was the case for our experiments. An attempt was made to fit the experimental data by re-calibrating a and a_d, yielding values larger than those used for H6, due to the shallower flow depth. The model predictions represented with reasonable agreement the measured flume 1 sediment concentrations for the three finest size classes (< 2, 2-20 and 20-50 μm) only when the mass of soil per unit area in the deposited layer, m_t^*, was also reduced to 2.5 mg cm^{-2} instead of 11 mg cm^{-2} (as used in H6). The reduction in m_t^* is consistent with the decreased rainfall intensity, i.e., less soil per unit area is needed to protect the original soil. The model could not reproduce satisfactorily the measured sediment concentrations of the mid- and larger size classes (50-100, 100-315, 315-1000 and > 1000 μm). It slightly over-predicted the total sediment concentration due to its failure to predict the long-time behavior of the larger particle classes. The estimated parameter and the modified settling velocities used in this procedure fitting are reported in Tables 2 and 3.

The results suggest that, for the low rainfall intensity of 28 mm h^{-1}, 2 h was insufficient to reach the steady-state behavior. Particularly for the larger particles, it is not obvious that constant steady-state effluent concentrations were reached at the end of the erosion event (Figure 6). It was observed

visually that for this event that topsoil compaction was reduced relative to H6 (no DTM was measured for this experiment). The question of steady-state conditions is addressed in §4.

To fit the experimental results collected from flume 2, the area-adjusted H-R model was used with the same parameter set as for flume 1, except for the value of a. Based on the steady discharge rate at the flume exit, it was estimated that, at steady state, the 40% rock fragment cover increased the overland flow depth to about 4 mm. Accordingly, the value of a was reduced (Table 2) to account for the increase in the overland flow depth compared with flume 1. The adjusted H-R model represented reasonably the short- and long-time behavior of the finer size classes observed in flume 1 (no rock fragments). However, the model could not reproduce the concentrations of the larger size classes or, in consequence, the total sediment concentration.

4. Discussion

The effect of rock fragment coverage on soil erosion and hydrological processes was investigated considering (i) soil surface coverage (with or without rock fragments) and (ii) different rainfall intensities (high and low precipitation rates). The same initial conditions were used in each experiment. Two different sediment size-dependent erosion time scales – short and long times – were used, which can be help to explain later the results:

- The experiments show for all sediment sizes an increase in sediment concentration to a maximum, followed by a decline. Since the deposited layer acts to protect the soil from erosion, it follows that the maximum sediment concentrations in the effluent are related to its formation. The time at which the peak occurs divides the short and long time scales. It varies little amongst the different sediment classes, but rather depends on the precipitation rate and rock fragment cover.

- Flume experiments consistently show that, relative to the grain-size distribution of the soil, effluent concentrations are enriched in finer materials, particularly at short times, since these particles settle more slowly than large particles [*Proffitt et al.*, 1991; *Durnford and King*,1993; *Malam Issa et al.*, 2006].
- At long times – meaning times after the sediment concentration peak – previous results show that the distribution of grain sizes in the effluent approaches that of the parent soil under net erosion conditions [*Walker et al.*, 1978; *Proffitt et al.*, 1991]. Physical explanations for this behavior are (i) the (assumed) non-selective erosion of particles from parent soil, and (ii) that the deposited layer is not complete and perhaps non-uniform, such that parts of the soil are protected from erosion, while in other parts the original soil undergoes continuous erosion.

Effect of Rock Fragment Cover on the Hydrological Response and Total Soil Erosion Delivery

In the experiments, rainfall was applied to an initially dry soil. Rock fragment cover had the effect of increasing the infiltration rate (relative to the bare soil), increasing the time-to-ponding and time-to-runoff, which in turn reduced the total soil erosion delivery. The increased infiltration rate is due to (i) the protection provided by the rock fragments against soil sealing/compaction, which reduces the soil's hydraulic conductivity, and (ii) the reduced cross-sectional area for surface flow, which led to an increased water depth on the surface, increasing the infiltration (e.g., [*Barry et al*., 1995]). Based on the deposition rate (§2.3.1), the deposited materials is proportional to the infiltration rate. This suggests that the presence of rock fragments increases the deposited materials in their vicinity, that is, where the infiltration is supposed higher (Figure 7). In addition, the presence of rock fragments on the topsoil decreased the overland flow velocity compared to the flume with bare soil (Table 2). Consequently, the runoff rate reduced due to the presence of rock fragments on the soil surface compared with the bare soil (Figure 3). These findings are summarized in Table 4, where it is

noted that the difference in overland flow depth between the bare and rock fragment-covered flumes varies with the time scale. Because the time-to-ponding is delayed for the rock fragment-covered flume, the water depth is less than that for the bare soil. However, when the overland flow is fully developed, the water depth is greater than for the bare soil (Table 2), despite the greater infiltration.

Table 4 near here

Effect of Rock Fragment Cover on the Effluent Sediment Concentration

Compared with the bare soil, the rock fragment cover produced different behavior for different sediment size classes. At short times, the contribution of the mid- and larger size classes (50-100, 100-315 and 315-1000 μm) to the total effluent sediment composition increased slightly compared with the finer size classes. For the latter, for given effective rainfall we suggest that the concentrations decreased proportionally to the area exposed during the entire erosion event (Figures 4 and 6). This behavior – the short-time increase of the mid- and larger-sized particle sediment concentrations due to the rock fragments − was more pronounced for high rainfall intensity and low rock fragment cover (Figure 4, experiment H6) than for low rainfall intensity and high rock fragment cover (Figure 6, experiment H7-E1). That is, while increasing water depth attenuates the raindrop impact, the force required to suspend the soil particles depends on grain size. *Koon et al.* [1970] reported that infiltration occurs mainly along the perimeter rather than beneath rock fragments. Thus, during the initial phase of the erosion event, water would move in both vertical and lateral directions (in uncovered areas). This would reduce the overland flow depth at the periphery of rock fragments retarding the raindrop attenuation and increasing the raindrop detachment compared with the bare soil. For mid- and larger-sized particles, *Mazurak and Mosher* [1968] and *Leguédois et al*. [2005] found that raindrop splash-induced motion is grain-size dependent, with a maximum for mid-size particles (50-1000 μm), consistent with the enrichment noted in the rock fragment-covered flume

effluent concentrations (measured sediment concentrations of size classes ranged in 50-1000 μm, Figure 4). For a given soil condition, raindrop impact and water depth (which varied between the flumes), fine particles are transported more easily than coarser particles [*Hogarth et al.*, 2004]. Results for the largest size class (> 1000 μm) showed considerable scatter, even though they appear to have a similar pattern to the other size classes. The scatter is attributed to different transport mechanisms, e.g., rolling over the bed or saltation, which are more likely to be manifested for larger particles, as mentioned above.

Effect of Rainfall Intensity

The experiments showed that sediment concentrations increased with increasing rainfall intensity. This observation applies to the total eroded mass, the peak concentration magnitude and the steady-state effluent concentrations (Figures 4 and 6). With high rainfall (experiment H6, Figure 4), the total sediment concentration peaked soon after runoff commenced and then declined rapidly to its steady-state value. The low rock fragment coverage (20%) and high rainfall led to similar overland flow depths, but nonetheless the data in Figure 4 show that the sediment concentrations are lower in all size classes except for the largest.

In experiment H7-E1 (Figure 6) − with a low rainfall rate and increased rock fragment cover (40%) − effluent sediment concentrations were different for all size classes. The main impact, compared with experiment H6 (Figure 4), is that the initial sediment peak concentration was delayed, with lower concentrations, the latter occurring because erosion is directly proportional to the precipitation rate. Thus, there was less suspended sediment eroded at early times (Figure 6) which retarded the deposited layer formation (and, hence, the timing of the peak concentration in the effluent). This effect is counterbalanced, partially at least, because the amount of deposition needed to

form the shield layer is dependent on the precipitation rate [*Sander et al.*, 1996]. This result becomes evident in the application of the H-R model to the data, discussed below.

Grain-Size Distribution of the Original Soil and Effluent

Previous experimental results have revealed that, at steady state, flume sediment concentrations are in proportion to the original soil's grain-size distribution [*Walker et al.*, 1978; *Moss and Green*, 1983; *Proffitt et al.*, 1991; *Tromp-van Meerveld et al.,* 2008]. This behavior is a feature of the H-R model [*Hairsine and Rose*, 1991, *Sander et al.*, 1996]. However, in both experiments reported here, the sediment effluent concentrations, although consistent for bare/rock fragment-covered flume pair, were different to the original soil. The finer grain sizes, in particular, were lower in the original soil. The results showed consistent behavior in terms of steady-state sediment effluent concentrations between flumes with and without rock fragments when the same rainfall intensity was used. However, they showed inconsistent behavior when different precipitation rates were used (Table 3). This difference is attributed to the effect of the precipitation rate on soil sealing or soil cohesion (see *Assouline* [2004] for a review). It is possible that the change in soil cohesion is due in part to soil aggregate breakdown, which is not accounted for in the H-R model. We observed that soil aggregates, present on the surface initially, were broken down differently during the rainfall events. This behavior has been observed previously [*Misra and Rose*, 1995; *Legout et al.*, 2005]. Additionally, (6) shows that the time scale to reach steady-state effluent sediment concentrations depends on class size. Thus, the largest particles (largest v_i) take the longest time to reach equilibrium behavior. For instance, the steady-state behavior during the experiment H6 required at least 0.76 h and 0.80 h for flumes with and without rock fragments, respectively. However, using the lower rainfall intensity for the H7-E1 experiment results in slightly shorter times being needed to meet the equilibrium behavior, which is evaluated by 0.60 h and 0.49 h for flumes 1 and 2, respectively for the largest size particles (Table 5).

Intuitively, lower rainfall intensities need longer time to reach steady state than higher rainfall precipitations as explained previously. The discrepancy between what was expected and what was found in terms of the characteristic time needed to achieve steady-state conditions for experiment H7-E1 could perhaps be explained by the somewhat unrealistic model parameters estimated during the calibration. In fact, it was found that the H-R model calibration did not lead to physically reasonable parameters for the low rainfall intensity experiment (H7-E1).

Table 5 near here

Effect of Rock Fragments on Change in the Soil Surface Elevation

It was observed for experiment H6 (Figure 8a) that the elevation change of the rock fragment-covered flume was greater than for the bare flume. This change is due to both erosion and compaction, both of which differ for each flume. The different amounts of compaction are due to the greater water infiltration into the rock fragment-covered flume (Figures 3 and 5). The prepared (by hand cultivation and smoothing) soil in each flume was initially relatively dry, with a relatively low bulk density. The influent water acts a lubricant [*Hillel*, 2004], and is present over a greater depth of the soil profile in the rock fragment-covered flume, leading to increased soil compaction compared with the bare flume. Compaction was possibly facilitated to some extent by vibrations generated by the sprinklers. In the overlapping lines, the compaction was the same for both flumes (Figures 2 and 8b); even though the moisture content differed. It seems that, in this region, the optimal moisture content needed to reach the maximum compaction under the experimental conditions was achieved in both flumes (Figure 5). Soil erosion differed between the flumes also. *Jomaa et al.* [2012] reported that the total eroded mass for flumes 1 and 2 for experiment H6 was around 7.1 and 4.3 kg m^{-1}, respectively. These values correspond to an average loss per unit area of 1.2 and 0.72 kg m^{-2} of the original soil. Using the initial measured bulk density (1110 kg m^{-3}), it was calculated that this soil

removal reduced on average the elevation of original soil by about 1.8 and 1.1 mm for flumes 1 and 2, respectively. However, in the flume with rock fragments, only the exposed area (that is, not covered by rock fragments) can be eroded. The predicted eroded mass accounting for the entire exposed soil to raindrop detachment (with rock fragment cover) is about 1.4 mm, still smaller than the corresponding value for flume 1. The additional overburden weight generated by the presence of the rock fragments on the soil surface might have induced additional compaction compared with the bare soil flume, although this is unlikely to be significant.

H-R Model Fitting

The H-R model fitting of the data helped gain further insights into the mechanisms that control soil erosion in the different conditions considered. The H-R model includes, as input information, the proportion of the soil within each sediment class size; these proportions being determined from the particle size distribution of the original soil. As already reported above, for the experiment H6, the flume data did not reach this end-point (original soil proportion), even though steady effluent concentrations were reached for nearly all the size classes by the end of the 3-h experiment (Table 3). The H-R model was applied using the proportions determined from the effluent concentration data. For experiment H6 (high rainfall intensity of 74 mm h^{-1} and low rock fragment cover of 20%), the H-R model reproduced well ($r^2 > 0.93$) the three finest size classes (> 2, 2-20 and 20-50 μm), but was less satisfactory for the remaining size classes (up to 1000 μm, $r^2 > 0.69$, Figure 4).

For the low rainfall intensity cases (experiment H7-E1, Figure 6), the experimental results overall were not reproduced satisfactorily by the model, particularly in the presence of rock fragments. Note that in the following discussion the largest size class was not considered due to the large scatter and lack of a clear pattern (again, this is due to irregular particle motions ignored by the H-R model). For

flume 1, an acceptable comparison between model and experiment was achieved for the three finest size classes (r^2 = 0.84), while the mid- and coarse particles only a lower correlation could be obtained (r^2 = 0.34). The reasons for the weak model performance for low rainfall are not clear. One possibility is that low rainfall extends the time needed for compaction, increasing the time needed to seal the surface while also a lower and more spatially variable overland flow depth is produced. The former could result in changes in the soil erodibility (due to changes in cohesion), and the latter would increase the raindrop-induced delivery [*Misra and Rose*, 1995]. Rainfall-induced compaction of the bed and soil surface sealing are not included in the H-R model.

In terms of the H-R model itself, a sensitivity analysis revealed that results are significantly affected by values of the settling velocities and the overland flow depth, as previously found by *Sander et al.* [1996] and *Tromp-van Meerveld et al*. [2008]. During the fitting of experiment H6 (high rainfall intensity), for the four finest size classes, the settling velocities measured in separate experiments were used (see *Tromp-van Meerveld et al.* [2008] and *Jomaa et al.* [2010] for details). However, as found previously, for the coarser size classes the settling velocities had to be adjusted to a value smaller than the measured range to obtain a reasonable model comparison (Table 3). Physically speaking, it is not surprising that the model results are sensitive to settling velocities and water depth. Raindrop-induced erosion is attenuated by increasing overland flow depth, and varies rapidly over the range of a few raindrop diameters. In our experiments, the raindrops were about 2.2 mm in diameter, while the overland flow depth for the low-precipitation experiment was about 3-4 mm on average. In addition to this, the sedimentation rate of the mid- and large-size classes is affected by hindered settling [*Richardson and Zaki*, 1954; *Baldock et al.*, 2004]. Grain-to-grain collisions, which are more likely in shallow water layers, reduce the settling velocity. For example, *Baldock et al.* [2004] found the velocity was reduced by a factor of two in laboratory tube

experiments. Additionally, the H-R model considers raindrop detachment as non-selective process, which is inconsistent with the experimental results as explained above. This affects the physical meaning of the model parameters, in particular the settling velocity (Table 3). The settling velocities for the larger size classes had to be estimated and are smaller than the measured values.

Hogarth et al. [2004] determined that the characteristic settling velocity, $v_c = a_d RD / m_t^*$, can be used to ascertain whether a particle within the overland flow tends to remain suspended within it. Particles for which $v_i < v_c$ tend to remain in the flow. Due to settling, particles in the flow are more retarded, on average, relative to the mean overland flow rate, as v_i increases. For experiment H6, v_c was estimated as 2.08×10^{-3} m s^{-1}. According to the v_c calculation, the two finest size classes (< 2 and 2-20 μm) move suspended within the flow and they are quite insensitive to changes in overland flow characteristics, especially the depth. On the other hand, the largest size class (> 1000 μm) is characterized by a high settling velocity (at least 10^2 greater than the characteristic settling velocity), and thus these sediments move due to raindrop impact and via rolling motions [*Asadi et al.*, 2007]. In addition, we calculated the Rouse number [*Rouse*, 1950], which indicated that non-suspended load transport would occur for v_i larger than about 5×10^{-2} m s^{-1}. Table 3 shows that at least the largest particle size class would be transported as non-suspended sediment for both experiments, and that the experimental conditions likely induced a transition between suspended-load transport and other mechanisms. In consequence, the motion of the intermediate size classes is sensitive to the local hydraulic conditions. The fitted settling velocities in Table 3 suggest that this sensitivity is increased for the low rainfall case (experiment H7-E1).

5. Conclusions

Two experiments were conducted at the EPFL erosion flume to test the effect of rock fragments on the concentrations of the individual size classes and the hydrological response. The effect of two rock fragment coverages (20 and 40%) was tested under two rainfall intensities (28 and 74 mm h^{-1}) with a gentle slope (2.2%). The experiments were conducted with prepared soils (the soil surface was smoothed then covered by rock fragments having the same size and were uniformly distributed). Results showed that the rock fragments have a selective effect on the size of sediment that is eroded from the flume. Compared with bare soil, rock fragments lead to an increased overland flow depth, the size-selective effect of which can be related to sediment erosion time scales. For short times (before the sediment concentration peak), the rock fragments provide greater protection to the finer particles (< 2 and 2-20 20-50 and 50-100 μm) but, as the particle size increases, the protection decreases. The magnitude of this effect is proportional to the rock fragment coverage and rainfall intensity, i.e., greater rock fragment coverage provides greater protection. However, for the larger size classes (100-315, 315-1000 and > 1000 μm), the rock fragments did not provide any protection. At long times (steady state), it seems that the rock fragments reduce the sediment concentration of the individual size classes equally without any preference. We suggest that this is due to the overland flow depth increasing and so attenuating the raindrop detachment. A possible explanation of the early selective effect of rock fragments is that the analysis assumed steady flow, but this is not correct at early times. Again, this effect is proportional to the effective rainfall intensity and rock fragment cover.

The H-R erosion model was adjusted for taking the effects of rock fragment cover on soil erosion into account. This was done by suitably adjusting the parameters based on the area not covered by rock fragments. It was found that the modified H-R model predictions reproduced well the total and

the individual size classes of experiment H6 (high rainfall intensity and low rock fragment cover). However, the H-R model could not represent reasonably all individual and the total sediment concentrations of the experiment H7-E1 (for both flumes; with and without rock fragments). The model does not account for surface sealing, aggregate breakdown or non-suspended load transport, all of which possibly occurred in the experiments.

Although experiments in this work were not replicated, the results presented here and in previous works using the same rainfall simulator (see for example *Tromp-van Meerveld et al.* [2008]; *Jomaa et al.* [2010, 2012]) provide consistent datasets, comprising more than 20 experiments conducted on the same soil, and with precipitation rates in the same range (28-74 mm h^{-1}). These datasets give a clear picture of the erosion patterns and yields, as well as the degree of variability that can be expected. Based on this set of experiments, we concluded that, in the laboratory conditions adopted, the variability is limited, since we have good control over all the experimental variables (soil surface characteristics, rainfall distribution, slope, etc.). For these reasons, the data are viewed as reliable. The 1D modeling approach used does not account for bed morphology changes or changes in overland flow that occur during a rainfall event. Investigations with a more detailed model that relaxes these restrictions are planned, and will potentially lead to greater understanding on the role played by rock fragments on soil erosion processes.

Acknowledgments

This work was supported by the Swiss National Science Foundation (Grants 200021-113815 and 200020-132544/1).

References

Abrahams, A. D., and A. J. Parsons (1991), Relation between infiltration and stone cover on a semiarid hillslope, southern Arizona, *J. Hydrol.*, *122*(1-4), 49-59, doi:10.1016/0022-1694(91)90171-D.

Abrahams, A. D., and A. J. Parsons (1994), Hydraulics of interrill overland flow on stone-covered desert surfaces, *Catena*, *23*(1-2), 111-140, doi:10.1016/0341-8162(94)90057-4.

Adams, J. E. (1966), Influence of mulches on runoff erosion and soil moisture depletion, *Soil Sci. Soc. Am Proc.*, *30*(1), 110-114.

Asadi, H., H. Ghadiri, C. W. Rose, and H. Rouhipour (2007), Interrill soil erosion processes and their interaction on low slopes, *Earth Surf. Processes Landforms*, *32*(5), 711-724, doi:10.1002/esp.1426.

Assouline, S. (2004), Rainfall-induced soil surface sealing: A critical review of observations, conceptual models, and solutions, *Vadose Zone J.*, *3*(2), 570-591, doi: 10.2113/3.2.570

Baril, P. (1991), Erodibilité des sols et érodabilité des terres : Application au plateau vaudois, Ph.D. thesis, 218 pp., Ecole Polytech. Féd. de Lausanne (EPFL), Lausanne, Switzerland, doi:10.5075/epfl-thesis-940.

Barry, D. A., J.-Y. Parlange, R. Haverkamp, and P. J. Ross (1995), Infiltration under ponded conditions: 4. An explicit predictive infiltration formula, *Soil Sci*., *160*(1), 8-17.

Barry, D. A., G. C. Sander, S. Jomaa, B. C. P. Heng, J.-Y. Parlange, I. G. Lisle, and W. L. Hogarth (2010), Exact solutions of the Hairsine-Rose precipitation-driven erosion model for a uniform grain-sized soil, *J. Hydrol.*, *389*(3-4), 399-405, doi:10.1016/j.jhydrol.2010.06.016.

Baldock, T. E., M. R. Tomkins, P. Nielsen, and M. G. Hughes (2004), Settling velocity of sediments at high concentrations, *Coastal Eng.*, *51*(1), 91-100, doi:10.1016/j.coastaleng.2003.12.004.

Beuselinck, L., G. Govers, P. B. Hairsine, G. C. Sander, and M. Breynaert (2002), The influence of rainfall on sediment transport by overland flow over areas of net deposition, *J. Hydrol.*, *257*(1-4), 145-163, doi:10.1016/S0022-1694(01)00548-0.

Boyer, C., and A. G. Roy (1991), Morphologie du lit autour d'un obstacle soumis à un écoulement en couche mince, *Geogr. Phys. Quat.*, *45*(1), 91-99.

Bunte, K., and J. Poesen (1993), Effects of rock fragment covers on erosion and transport of noncohesive sediment by shallow overland flow, *Water Resour. Res.*, *29*(5), 1415-1424, doi:10.1029/92WR02706.

Bunte, K., and J. Poesen (1994), Effects of rock fragment size and cover on overland flow hydraulics, local turbulence and sediment yield on an erodible soil surface, *Earth Surf. Processes Landforms*, *19*(2), 115-135, doi:10.1002/esp.3290190204.

Cerdà, A. (2001), Effects of rock fragment cover on soil infiltration, interrill runoff and erosion, *Eur. J. Soil Sci.*, *52*(1), 59-68, doi:10.1046/j.1365-2389.2001.00354.x.

de Figueiredo, T., and J. Poesen (1998), Effects of surface rock fragment characteristics on interrill runoff and erosion of a silty loam soil, *Soil Tillage Res.*, *46*(1-2), 81-95, doi:10.1016/S0167-1987(98)80110-4.

De Ploey, J. (1981), Crusting and time-dependent rainwash mechanisms on loamy soil, *Soil conservation: Problems and prospects*, J. Wiley and Sons, Chichester (1981), 139-152.

Dermisis, D. C., and A. N. Papanicolaou (2010), Enhanced insight on the effects of boulders on bedload transport. *River Flow*, Dittrich, Koll, Aberle and Geisenhainer (eds), Bundesanstalt für Wasserbau ISBN 978-3-939230-00-7, pp. 855-861.

Durnford, D., and J. P. King (1993), Experimental study of processes and particle-size distributions of eroded soil, *J. Irrig. Drain. E.*, *119*(2), 383-398, doi: 10.1061/(ASCE)0733-9437(1993)119:2(383).

Elhakeem, M., and A. N. Papanicolaou (2009), Estimation of the runoff curve number via direct rainfall simulator measurements in the state of Iowa, USA. *Water Res. Manage.*, 23(12), 2455-2473, doi: 10.1007/s11269-008-9390-1.

Gao, B., M. T. Walter, T. S. Steenhuis, J.-Y. Parlange, B. K. Richards, W. L. Hogarth, and C. W. Rose (2005), Investigating raindrop effects on transport of sediment and non-sorbed chemicals from soil to surface runoff, *J. Hydrol.*, *308*(1-4), 313-320, doi:10.1016/j.jhydrol.2004.11.007.

Grant, G.E. (1997), Critical flow constrains flow hydraulics in mobile-bed streams: A new hypothesis. *Water Resour. Res.*, 33(2), 349-358, doi:10.1029/96WR03134.

Guo, T., Q. Wang, D. Li, and J. Zhuang (2010), Effect of surface stone cover on sediment and solute transport on the slope of fallow land in the semi-arid loess region of northwestern China, *J. Soils Sed.*, *10*(6), 1200-1208, doi:10.1007/s11368-010-0257-8.

Hairsine, P. B., and C. W. Rose (1991), Rainfall detachment and deposition-sediment transport in the absence of flow-driven processes, *Soil Sci. Soc. Am. J.*, *55*(2), 320-324, doi:10.2136/sssaj1991.03615995005500020003x.

Heng, B. C. P., G. C. Sander, A. Armstrong, J. Quinton, J. H. Chandler, and C. F. Scott (2011), Modeling the dynamics of soil erosion and size-selective sediment transport over non-uniform topography in flume-scale experiments. *Water Resour. Res.*, *47*, W02513, doi:10.1029/2010WR009375.

Heng, B. C. P., G. C. Sander, and C. F. Scott (2009), Modeling overland flow and soil erosion on nonuniform hillslopes: A finite volume scheme, *Water Resour. Res.*, *45*, W05423, doi:10.1029/2008WR007502.

Hillel, D. (2004), Introduction to environmental soil physics. *Elsevier Academic Press*, Amsterdam, Netherlands, 494 pp.

Hogarth, W. L., C. W. Rose, J.-Y. Parlange, G. C. Sander, and G. Carey (2004), Soil erosion due to rainfall impact with no inflow: A numerical solution with spatial and temporal effects of sediment settling velocity characteristics, *J. Hydrol.*, *294*(4), 229-240, doi:10.1016/j.jhydrol.2004.03.007.

IUSS Working Group WRB (2007), World Reference Base for Soil Resources 2006, first update 2007. World Soil Resources Reports No. 103. FAO, Rome, Italy, http://www.fao.org/fileadmin/templates/nr/images/resources/pdf_documents/wrb2007_red.pdf, last accessed 3 April 2012.

Jaffrain, J., A. Studzinski, and A. Berne (2011), A network of disdrometers to quantify the small-scale variability of the raindrop size distribution. *Water Resour. Res.*, *47*, doi:10.1029/2010WR009872.

Jean, J. S., K. F. Ai, K. Shih, and C. C. Hung (2000), Stone cover and slope factors influencing hillside surface runoff and infiltration: Laboratory investigation, *Hydrol. Processes*, *14*(10), 1829-1849, doi:10.1002/1099-1085(200007)14:10<1829::AID-HYP66>3.0.CO;2-#.

Jomaa, S., D. A. Barry, A. Brovelli, G. C. Sander, J.-Y. Parlange, B. C. P. Heng, and H. J. Tromp-van Meerveld (2010), Effect of raindrop splash and transversal width on soil erosion: Laboratory flume experiments and analysis with the Hairsine-Rose model, *J. Hydrol.*, *395*(1-2), 117-132, doi:10.1016/j.jhydrol.2010.10.021.

Jomaa, S., D. A. Barry, A. Brovelli, B. C. P. Heng, G. C. Sander, J.-Y. Parlange, and C. W. Rose (2012), Rain splash soil erosion estimation in the presence of rock fragments, *Catena*, *92*(1), 38-48, doi:10.1016/j.catena.2011.11.008.

Kinnell, P.I.A. (2005), Raindrop-impact-induced erosion processes and prediction: A review. *Hydrol. Processes*, *19*(14), 2815-2844,doi:10.1002/hyp.5788.

Koon, J. L., J. G. Hendrick, and R. E. Hermanson (1970), Some effects of surface cover geometry on infiltration rate, *Water Resour. Res.*, *6*(1), 246-253, doi:10.1029/WR006i001p00246.

Le Bissonnais, Y., Renaux, B., Delouche, H., 1995. Interactions between soil properties and moisture content in crust formation, runoff and interrill erosion from tilled loess soils. *Catena*, *25*(1-4), 33-46, doi:10.1016/0341-8162(94)00040-L.

Legout, C., S. Leguédois, and Y. Le Bissonnais (2005), Aggregate breakdown dynamics under rainfall compared with aggregate stability measurements, *Eur. J. Soil Sci.*, 56(2), 225-237, doi:10.1111/j.1365-2389.2004.00663.x.

Leguédois, S., O. Planchon, C. Legout, and Y. Le Bissonnais (2005), Splash projection distance for aggregated soils: Theory and experiment, *Soil Sci. Soc. Am. J.*, *69*(1), 30-37.

Lisle, I. G., C. W. Rose, W. L. Hogarth, P. B. Hairsine, G. C. Sander, and J.-Y. Parlange (1998), Stochastic sediment transport in soil erosion, *J. Hydrol.*, *204*(1-4), 217-230, doi:10.1016/S0022-1694(97)00123-6.

Loosvelt, L. (2007), Scale dependent influence of rock fragment cover on soil infiltration, runoff and sediment yield in arid zones of Chile, Ph.D. thesis, 155 pp., Universiteit Gent, Gent, Belgium.

Malam Issa, O., Y. L. Bissonnais, O. Planchon, D. Favis-Mortlock, N. Silvera, and J. Wainwright (2006), Soil detachment and transport on field- and laboratory-scale interrill areas: Erosion processes and the size-selectivity of eroded sediment, *Earth Surf. Processes Landforms*, *31*(8), 929-939, doi:10.1002/esp.1303.

Mandal, U. K., K. V. Rao, P. K. Mishra, K. P. R. Vittal, K. L. Sharma, B. Narsimlu, and K. Venkanna (2005), Soil infiltration, runoff and sediment yield from a shallow soil with varied stone cover and intensity of rain, *Eur. J. Soil Sci.*, *56*(4), 435-443, doi:10.1111/j.1365-2389.2004.00687.x.

Martinez-Zavala, L., and A. Jordan (2008), Effect of rock fragment cover on interrill soil erosion from bare soils in Western Andalusia, Spain, *Soil Use Manage.*, *24*(1), 108-117, doi:10.1111/j.1475-2743.2007.00139.x.

Martinez-Zavala, L., A. Jordan, N. Bellinfante, and J. Gil (2010), Relationships between rock fragment cover and soil hydrological response in a Mediterranean environment, *Soil Sci. Plant Nutr.*, *56*(1), 95-104, doi:10.1111/j.1747-0765.2009.00429.x.

Mazurak, A. P., and P. N. Mosher (1968), Detachment of soil particles in simulated rainfall, *Soil Sci. Soc. Am. J.*, *32*(5), 716-719, doi:10.2136/sssaj1968.03615995003200050036x.

Misra, R. K., and C. W. Rose (1995), An examination of the relationship between erodibility parameters and soil strength, *Aust. J. Soil Res.*, *33*(4), 715-732, doi:10.1071/SR9950715.

Moore, D. C., and M. J. Singer (1990), Crust formation effects on soil erosion processes, *Soil Sci. Soc. Am. J.*, *54*(4), 1117-1123, doi:10.2136/sssaj1990.03615995005400040033x.

Morgan, R. P. C., (2005), Soil erosion and conservation, *3rd edition*, *Blackwell Science Ltd.,* Oxford, United Kingdom, 304 pp.

Morgan, R. P. C., J. Quinton, and R. J. Rickson (1990), Structure of the soil erosion prediction model for the European Community. In Proceedings of the International Symposium on Water Erosion, *Sedimentation and Resource Conservation*, Central Soil and Water Conservation Research and Training Institute. Dehradun, India, pp. 49-59.

Morgan, R. P. C., J. Quinton, R. E. Smith, G. Govers, J. Poesen, K. Auerswald, G. Chisci, D. Torri, and M. E. Styczen (1998), The European Soil Erosion Model (EUROSEM): A dynamic approach for predicting sediment transport from fields and small catchments, *Earth Surf. Processes Landforms*, *23*(6), 527-544, doi:10.1002/(SICI)1096-9837(199806)23:6<527::AID-ESP868>3.0.CO;2-5.

Moss, A. J., and P. Green (1983), Movement of solids in air and water by raindrop impact. Effects of drop-size and water-depth variations, *Aust. J. Soil Res.*, *21*(3), 257-269, doi:10.1071/SR9830257.

Nearing, M. A., G. R. Foster, L. J. Lane, and S. C. Finkner (1989), A process-based soil erosion model for USDA-water erosion prediction project technology, *Trans. ASAE*, *32*(5), 1587-1593.

Papanicolaou, A. N., D. C. Dermisis, and M. Elhakeem (2011), Investigating the role of clasts on the movement of sand in gravel bed rivers, *J. Hydraul. Eng.*, 137(9), 871-784. doi:10.1061/(ASCE)HY.1943-7900.0000381.

Papanicolaou, A. N., and C. Kramer (2005), The role of relative submergence on cluster microtopography and bedload predictions in mountain streams, *Proc. Int. Symp. River*, Coastal, and Estuarine Morphodynamics, Taylor and Francis, London, United Kingdom, pp 1083-1086.

Parlange, J.-Y., W. L. Hogarth, C. W. Rose, G. C. Sander, P. Hairsine, and I. Lisle (1999), Addendum to unsteady soil erosion model, *J. Hydrol.*, *217*(1-2), 149-156, doi:10.1016/S0022-1694(99)00012-8.

Poesen, J., and F. Ingelmo-Sanchez (1992), Runoff and sediment yield from topsoils with different porosity as affected by rock fragment cover and position, *Catena*, *19*(5), 451-474, doi:10.1016/0341-8162(92)90044-C.

Poesen, J., and H. Lavee (1994), Rock fragments in top soils: Significance and processes, *Catena*, *23*(1-2), 1-28, doi:10.1016/0341-8162(94)90050-7.

Poesen, J., F. Ingelmo-Sanchez, and H. Mucher (1990), The hydrological response of soil surfaces to rainfall as affected by cover and position of rock fragments in the top layer, *Earth Surf. Processes Landforms*, *15*(7), 653-671, doi:10.1002/esp.3290150707.

Poesen, J., E. De Luna, A. Franca, J. Nachtergaele, and G. Govers (1999), Concentrated flow erosion rates as affected by rock fragment cover and initial soil moisture content, *Catena*, *36*(4), 315-329, doi:10.1016/S0341-8162(99)00044-2.

Poesen, J., D. Torri, and K. Bunte (1994), Effects of rock fragments on soil-erosion by water at different spatial scales - A review, *Catena*, *23*(1-2), 141-166, doi:10.1016/0341-8162(94)90058-2.

Poesen, J., B. van Wesemael, K. Bunte, and A. S. Benet (1998), Variation of rock fragment cover and size along semiarid hillslopes: A case-study from southeast Spain, *Geomorphology*, *23*(2-4), 323-335, doi:10.1016/S0169-555X(98)00013-0.

Poesen, J., and H. Lavee (1991), Effects of size and incorporation of synthetic mulch on runoff and sediment yield from interrills in a laboratory study with simulated rainfall, *Soil Tillage Res.*, *21*(3-4), 209-223, doi:10.1016/0167-1987(91)90021-O.

Proffitt, A. P. B., C. W. Rose, and P. B. Hairsine (1991), Rainfall detachment and deposition-experiments with low slopes and significant water depths, *Soil Sci. Soc. Am. J.*, *55*(2), 325-332.

Richardson, J. F., and W. N. Zaki (1954), Sedimentation and fluidization: Part 1, *Trans. Inst. Chem. Eng.*, *32*(1), 35-53.

Rieke-Zapp, D., J. Poesen, and M. A. Nearing (2007), Effects of rock fragments incorporated in the soil matrix on concentrated flow hydraulics and erosion, *Earth Surf. Processes Landforms*, *32*(7), 1063-1076, doi:10.1002/esp.1469.

Rouse, H., (1950). Engineering hydraulics, *John Wiley and Sons*, New York, USA, 1039 pp.

Rose, C. W. (1960), Soil detachment caused by rainfall, *Soil Sci.*, *89*(1), 28-35.

Rose, C. W. (1962), Some effects of rainfall, radiant drying, and soil factors on infiltration under rainfall into soils, *J. Soil Sci., 13*(2), 286-298, doi:10.1111/j.1365-2389.1962.tb00708.x.

Rose, C. W., J. R., Williams, G. C., Sander, D. A., Barry, (1983a), A mathematical model of soil erosion and deposition processes: I. Theory for a plane land element, *Soil Sci. Soc. Am. J.*, *47*(5), 991-995, doi:10.2136/sssaj1983.03615995004700050030x.

Rose, C. W., J. R., Williams, G. C., Sander, D. A., Barry, (1983b), A mathematical model of soil erosion and deposition processes: II. Application to data from an arid-zone catchment, *Soil* Sci. Soc. Am. J., 47(5), 996-1000, doi:10.2136/sssaj1983.03615995004700050031x.

Rose, C. W., W. L. Hogarth, G. Sander, I. Lisle, P. Hairsine, and J.-Y. Parlange (1994), Modeling processes of soil erosion by water, *Trends Hydrol.*, *1*, 443- 451.

Rose, C. W., B. Yu, H. Ghadiri, H. Asadi, J.-Y. Parlange, W. L. Hogarth, and J. Hussein (2007), Dynamic erosion of soil in steady sheet flow, *J. Hydrol.*, *333*(2-4), 449-458, doi:10.1016/j.jhydrol.2006.09.016.

Sander, G. C., J.-Y. Parlange, D. A. Barry, M. B. Parlange, and W. L. Hogarth (2007), Limitation of the transport capacity approach in sediment transport modeling, *Water Resour. Res.*, *43*(2), doi:10.1029/2006WR005177.

Sander, G. C., P. B. Hairsine, C. W. Rose, D. Cassidy, J.-Y. Parlange, W. L. Hogarth, and I. G. Lisle (1996), Unsteady soil erosion model, analytical solutions and comparison with experimental results, *J. Hydrol.*, *178*(1-4), 351-367, doi:10.1016/0022-1694(95)02810-2.

Sander, G. C., T. Zheng, P. Heng, Y. Zhong, and D. A. Barry (2011). Sustainable soil and water resources: Modelling soil erosion and its impact on the environment. *MODSIM 2011 - 19th International Congress on Modelling and Simulation - Sustaining Our Future: Understanding and Living with Uncertainty*. Perth, Western Australia, Australia, 12 – 16 December, 2011, pg. 45-56, http://www.mssanz.org.au/modsim2011/Plenary/sander.pdf, last accessed 3 April 2012.

Smets, T., J. Poesen, and E. Bochet (2008), Impact of plot length on the effectiveness of different soil-surface covers in reducing runoff and soil loss by water, *Prog. Phys. Geogr.*, *32*(6), 654-677, doi:10.1177/0309133308101473.

Torri, D., J. Poesen, F. Monaci, and E. Busoni (1994), Rock fragment content and fine soil bulk-density, *Catena*, *23*(1-2), 65-71, doi:10.1016/0341-8162(94)90053-1.

Tromp-van Meerveld, H. J., J.-Y. Parlange, D. A. Barry, M. F. Tromp, G. C. Sander, M. T. Walter, and M. B. Parlange (2008), Influence of sediment settling velocity on mechanistic soil erosion modeling, *Water Resour. Res., 44*(6), doi:10.1029/2007WR006361.

van Wesemael, B., J. Poesen, C. S. Kosmas, N. G. Danalatos, and J. Nachtergaele (1996), Evaporation from cultivated soils containing rock fragments, *J. Hydrol.*, *182*(1-4), 65-82, doi:10.1016/0022-1694(95)02931-1.

van Wesemael, B., J. Poesen, and T. de Figueiredo (1995), Effects of rock fragments on physical degradation of cultivated soil by rainfall, *Soil Tillage Res.*, *33*(3-4), 229-250, doi:10.1016/0167-1987(94)00439-L.

Veihe, A., J. Quinton, and J. Poesen, (2000), Sensitivity analysis of EUROSEM using Monte Carlo simulation II: the effect of rills and rock fragments. *Hydrol. Processes*, *14*(15), 927-939, doi:10.1002/(SICI)1099-1085(20000415)14:5<927::AID-HYP979>3.0.CO;2-V.

Viani, J.-P. (1986), Contribution à l'étude expérimentale de l'érosion hydrique, Ph.D. thesis, 239 pp. Ecole Polytech. Féd. de Lausanne (EPFL), Lausanne, Vaud, Switzerland, doi:10.5075/epfl-thesis-641.

Walker, P. H., P. I. A. Kinnell, and P. Green (1978), Transport of a noncohesive sandy mixture in rainfall and runoff experiments, *Soil Sci. Soc. Am. J.*, *42*(5), 793-801, doi:10.2136/sssaj1978.03615995004200050029x.

Woolhiser, D. A., R. E. Smith, and D. C. Goodrich (1990), KINEROS, a kinematic runoff and erosion model: Documentation and user manual, *U. S. Department of Agriculture, Agriculture Research Services, ARS-77* 130 pp., http://www.tucson.ars.ag.gov/kineros/, last accessed 23 February 2011.

Yager, E.M., J. W. Kirchner, and W. E. Dietrich (2007), Calculating bed load transport in steep boulder bed channels. *Water Resour. Res., 43*(7), doi:10.1029/2006WR005432.

Table 1. Summary of previous experiments on the effect of rock fragments on hydrological responses and soil erosion yields.

Reference	Experimental description	Initial moisture content (%)	Rock fragment characteristics			Effect on:				Conclusions
			Surface coverage (%)	Position	Size	Runoff	Infiltration rate	Soil erosion	Other	
Poesen et al. [1990]	Rainfall experiments were conducted at the laboratory scale	Topsoil (3 cm) was air-dried	20, 34, 49, 65, 83	Resting on the soil surface	3.3 × 7.0 × 10.3 cm	Decreased	Increased (into the unsealed soil surface)	-	Time-to-runoff increased	The rock fragments' position affects the hydrological response. Their effect is controlled by coverage proportion
				Embedded		Increased	Decreased (due to significant surface sealing)	-	Time-to-runoff decreased	
Poesen and Lavee [1991]	Rainfall simulator was used to carry out experiments using different mulch coverages	Air-dried	30, 49, 70, 88	Two cases were investi-gated (i) resting on the soil surface and (ii) partially embedded	Artificial mulches of 2 × 3 × 3 cm	The probability of overland flow generation in the vicinity of a rock fragment increases with increasing rock fragment size as does the probability of interrill soil loss	The infiltration rate decreased when the size of the mulch increased	Decreased exponentially with increasing mulch coverage	Mulch on the soil surface is more effective in reducing the runoff and sediment loss than if partially incorporated into it	Larger rocks are less efficient in reducing interrill soil loss
					Mulches in the range: 2 × 5.9 × 5.9 - 2 × 11.7 × 11.7 cm			Reduction was less pronounced and irregular		
					Mulches 2 × 22.3 × 22.3 cm			No significant effect when mulch cover was greater than 70%		
Poesen et al. [1994], *Poesen and Ingelmo-Sanchez* [1992], *de Figueiredo and Poesen* [1998]	Microplot scale (4×10^{-6} m^2), a single rock fragment	-	-	-	-	-	-	Decreased	Rock fragments protect the original soil against raindrop detachment	Ambivalent effects resulting from the soil type, porosity, slope, vertical position and size of rocks, as well as the occurrence of horseshoe vortex erosion
	Mesoplot scale (10^{-2} - 10^{2} m^2), area where the interrill erosion occurs			Resting on the soil surface or partially embedded		-	Increased	Decreased	The effect of rock fragments on soil erosion depends on the initial soil conditions and porosity (textural or structural)	
				Embedded		Increased distinct reticular flow (deeper and faster)	Decreased	Increased	The concentrated flow increased the detachment process and the transport capacity	
	Macroplot scale (10^{1} - 10^{4} m^2), area where rill and interrill erosion occur			-		-	-	Decreased	Exponential decrease with increasing rock fragment coverage	
Poesen et al. [1999]	Laboratory experiments were performed using a concentrated flow flume	Initially air-dry	0-75	Mixed into the soil matrix	Well-rounded ellipsoidal with inter-mediate axis in the range 0.5-1 cm	-	-	Increased	Rock fragments provide more protection to initially wet than to initially dry soils	Process-based erosion models should incorporate the effects of antecedent moisture content and rock fragment coverage
		Initially wet						Decreased		

Jean et al. [2000]	5% slope	The topsoil was initially wetted and compacted by sprinkling water and then air-dried	0, 10, 20 and 30	Resting on the soil surface	Gravel (0.95-2 cm)	Decreased when rock fragment cover increased	Increased	-	Raindrop interception and superficial water storage increased when the rock fragment cover increased independently	Variable and non-unique relationships between slope, rock fragment coverage, groundwater level, runoff, interception and superficial storage
	10% slope					Increased when rock fragment cover increased	Decreased	-		
	20% slope							-		
Cerdà [2001] Similar findings: *Mandal et al.,* [2005]; *Rieke-Zapp et al.,* [2007]; Martinez-*Zavala et al.,*[2008], [2010]; *Guo et al.,* [2010]	Field experiments with different initial conditions but same rainfall intensity (55 mm h^{-1})	In the range 1.7-3.7%	50-98	Resting on the soil surface	All particles greater than 2 mm resting on the soil surface	Decreased	Increased	Decreased	Rocks retard the overland flow ponding and enhance water percolation	Physically process-based erosion models should incorporate the rock fragments' effect especially in arid climates
Jomaa et al., [2012]	Flume laboratory experiments using different precipitations and rock fragment coverage	Range of 6.52-26.36%	20 and 40%	Resting on the soil surface	5-7 cm	Reduced	Increased	Decreased	In carefully controlled experiments, soil erosion was proportional to soil surface area exposed to raindrops. However, this finding was not confirmed using field data	The relationship soil erosion/area exposed was controlled to smaller extent by soil's initial moisture content, bulk density and soil surface characteristics

Table 2. Best-fit parameters obtained by fitting the experimental data sets H6 and H7-E1. The H-R model parameters for one of the experiments (carried out using the same flume and initial conditions but with different rainfall intensity) reported in *Jomaa et al.* [2010] are shown for comparison. In each experiment, flume 1 was bare soil and flume 2 had rock fragment coverage.

Experiments[a]	Flume	t_{ss}[c] (min)	v[d] (m min^{-1})	R (mm h^{-1})	D (mm)	Fr[e]	a (mg cm^{-3})	a_d (mg cm^{-3})	m_t^* (mg cm^{-2})	z (mm)	r^2	
											> 2, 2-20 and 20-50 µm	50-100, 100-315 and 315-1000 µm
H6 (20%)	1	16	0.76	68.70	9	0.04	10.0	8000	11.0	0.067	0.930	0.775
	2	21	0.61	54.40	11	0.03	7.0				0.962	0.692
H7-E1 (40%)	1	45	0.70	20.46	3	0.07	12.0	28000	2.5	0.015	0.873	0.405
	2	80	0.56	14.56	4	0.04	5.5				0.845	0.341
Flumes 1, 2[b]		-	-	48.00	9	-	27.0	9320	9.0	0.055	0.899[f]	

[a] Rock fragment cover in flume 2, while flume 1 is bare soil

[b] From *Jomaa et al.* [2010] where measured settling velocities were used (measured v_i)

[c] Time required to reach steady-state discharge rates. Before these times, the overland flow depth varied with space and time

[d] Average flow velocity

[e] Froude number ($Fr = v/(gD)^{1/2}$, where g is the magnitude of gravitational acceleration and D is the water depth)

[f] Value determined for the total sediment concentration

Table 3. Overview of the seven particle size diameter classes with their proportions measured in the original soil and in the effluent at the steady-state behavior for each experiment. Also, the measured settling velocities for all size classes were reported by *Tromp-van Meerveld et al.* [2008]. The measured settling velocities used are average values of the ranges reported (values shaded in light gray). The model-derived best-fit values are shaded in dark gray.

Size	Diameter (μm)		Proportion, p_i (%)					Settling velocity, v_i (m s^{-1})		v_i (m s^{-1})[a]	v_i (m s^{-1})	Nature of the
				H6 (74 mm h^{-1})		H7-E1 (28 mm h^{-1})						
Class	From	To	Original soil	Flume 1	Flume 2	Flume 1	Flume 2	From	To	used in H6	used in H7-E1	motion[b]
1	0	2	3.7	5.57	4.03	8.90	7.86	8.0×10^{-8}	4.0×10^{-6}	5.0×10^{-7}	8.0×10^{-8}	With the flow
2	2	20	19.4	22.32	23.57	49.87	45.38	4.0×10^{-6}	4.0×10^{-4}	1.5×10^{-5}	4.0×10^{-6}	With the flow
3	20	50	8.3	11.17	13.40	12.93	12.84	4.0×10^{-4}	2.5×10^{-3}	7.0×10^{-4}	8.0×10^{-4}	Depending on *D*
4	50	100	8.7	14.42	14.04	3.70	4.16	2.5×10^{-3}	1.4×10^{-2}	4.0×10^{-3}	8.0×10^{-2}	Depending on *D*
5	100	315	17.7	19.31	18.09	11.58	14.81	1.4×10^{-2}	3.7×10^{-2}	4.0×10^{-3}	4.0×10^{-2}	Depending on *D*
6	315	1000	20.3	13.24	12.08	7.82	10.96	3.7×10^{-2}	6.9×10^{-2}	4.0×10^{-3}	7.0×10^{-2}	Settle immediately
7	> 1000		21.3	13.97	14.79	5.20	3.99	6.9×10^{-2}	1.4×10^{-1}	6.0×10^{-2}	6.0×10^{-1}	Settle immediately

[a] *Jomaa et al.* [2010]

[b] Based on the criterion of *Hogarth et al.* [2004]

Table 4. Effect of rock fragments on soil erosion and hydrological processes compared with the bare soil. Summary of findings.

Time scale	Infiltration rate		Time-to-ponding and time-to-runoff		Overland flow depth		Runoff		Sediment concentration			
									Finer size classes		Mid- and larger size classes	
	Effect	Explanation	Effect	Explanation	Effect	Explanation	Effect	Explanation	Effect	Explanation	Effect	Explanation
Short times	Increased	Unsealed surface around and under the rock fragments	Increased	Increased flow meandering and infiltration rate	Decreased	Increased infiltration rate	Decreased	Increased infiltration rate	Decreased	Reduced area exposed	Increased	Delayed of water depth initiating
Long times	Increased	Increased overland water depth	-	-	Increased	Reduction of cross-sectional area	Decreased		Decreased		Decreased	Reduced area exposed

Table 5. Characteristic minimum time needed to achieve steady-state behavior for each size class as calculated from (6) [*Parlange et al.*, 1999]. The v_i used here are the averaged measured settling velocities reported in Table 3.

Size Class	Characteristic time t_0 (h)			
	H6		H7-E1	
	Flume 1	Flume 2	Flume 1	Flume 2
1	0.13	0.16	0.14	0.16
2	0.13	0.16	0.14	0.16
3	0.14	0.17	0.15	0.16
4	0.18	0.20	0.18	0.18
5	0.34	0.37	0.30	0.27
6	0.55	0.59	0.45	0.38
7	0.76	0.80	0.60	0.49

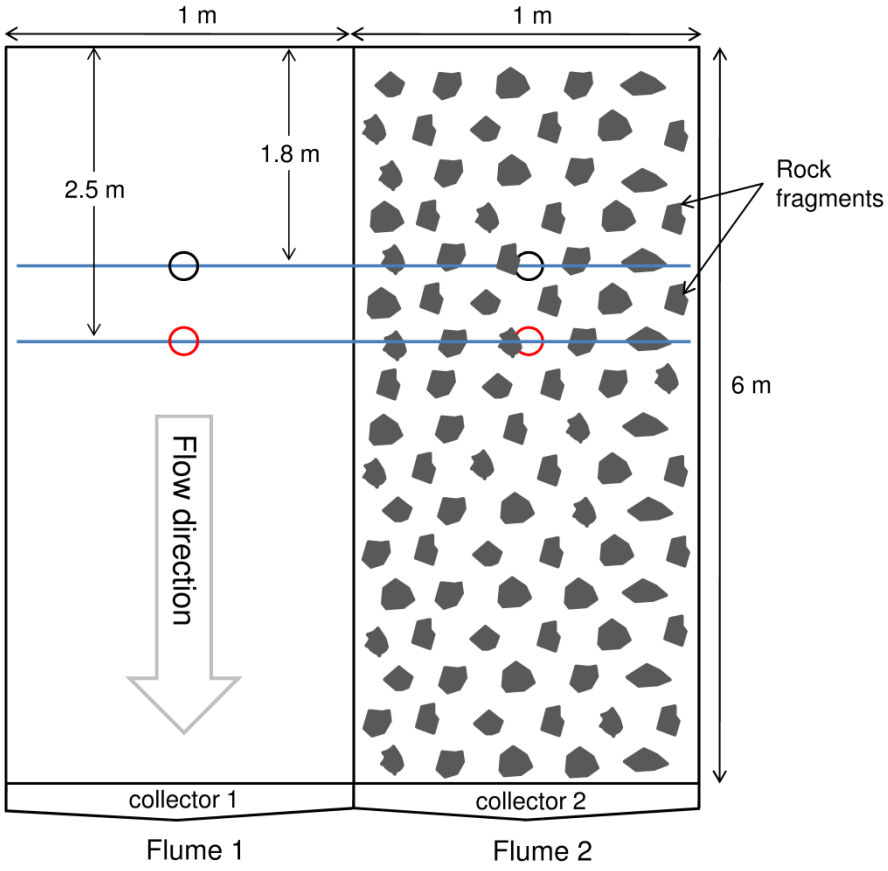

Figure 1. Overview of the experiment. The 6-m × 2-m EPFL erosion flume [*Tromp-van Meerveld et al.,* 2008; *Jomaa et al.,* 2010, 2012] was divided into two identical 1-m wide flumes. The soil surface of flume 1 remained bare, while flume 2 was covered with fluvial rock fragments. The horizontal blue lines located at 1.8 and 2.5 m from flume upstream indicate the cross sections where soil surface changes were examined (results reported in Figure 8). The open circles indicate the position where moisture content probes were embedded in the flumes. The red circle corresponds to the location where the moisture content measurement occurred on the sprinkler overlapping lines (Figure 2).

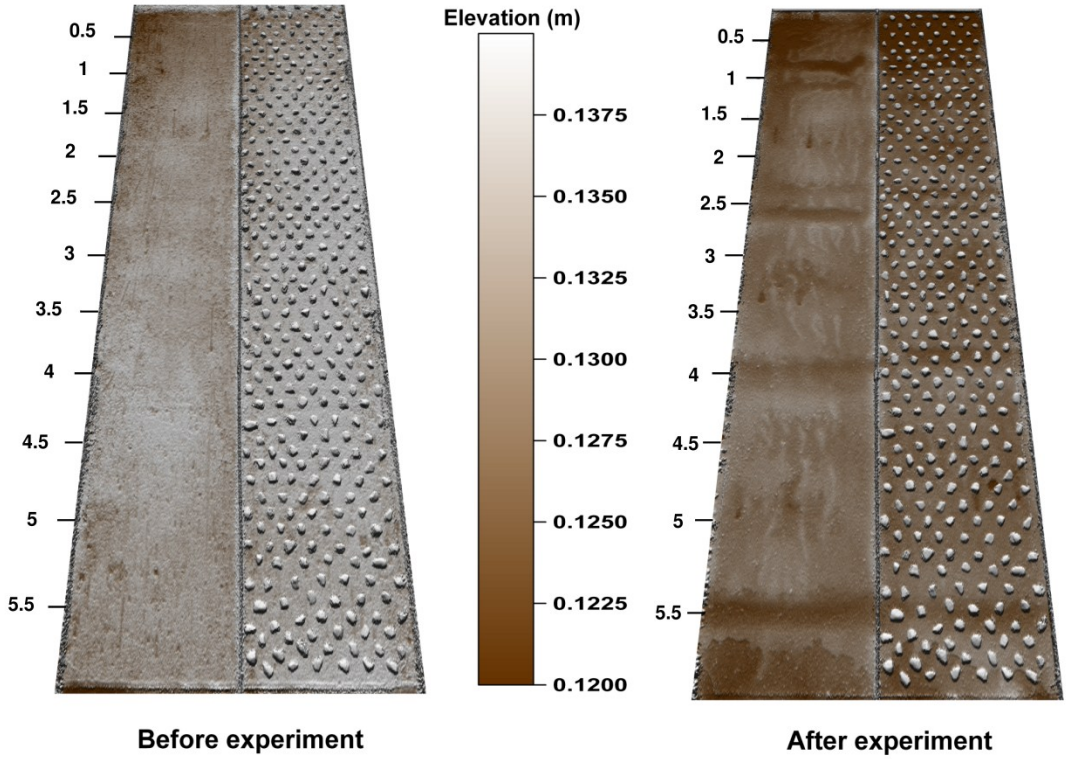

Figure 2. The soil surface elevation was mapped using a laser scanner before and after the experiment H6. Flumes 1 and 2 are separated by a vertical 10-cm high barrier. The numbers along the left side of each flume show the soil spatial location in the flumes (units: m). The digital terrain models (DTM's were corrected for slope) before the experiment illustrate that the soil surface was homogeneous, whereas after the experiment different erosion patterns appear with and without rock fragment coverage. The four dark brown horizontal lines visible in both flumes in the "After experiment" image (at about 1, 2.5, 4 and 5.5 m) are due to overlapping precipitation.

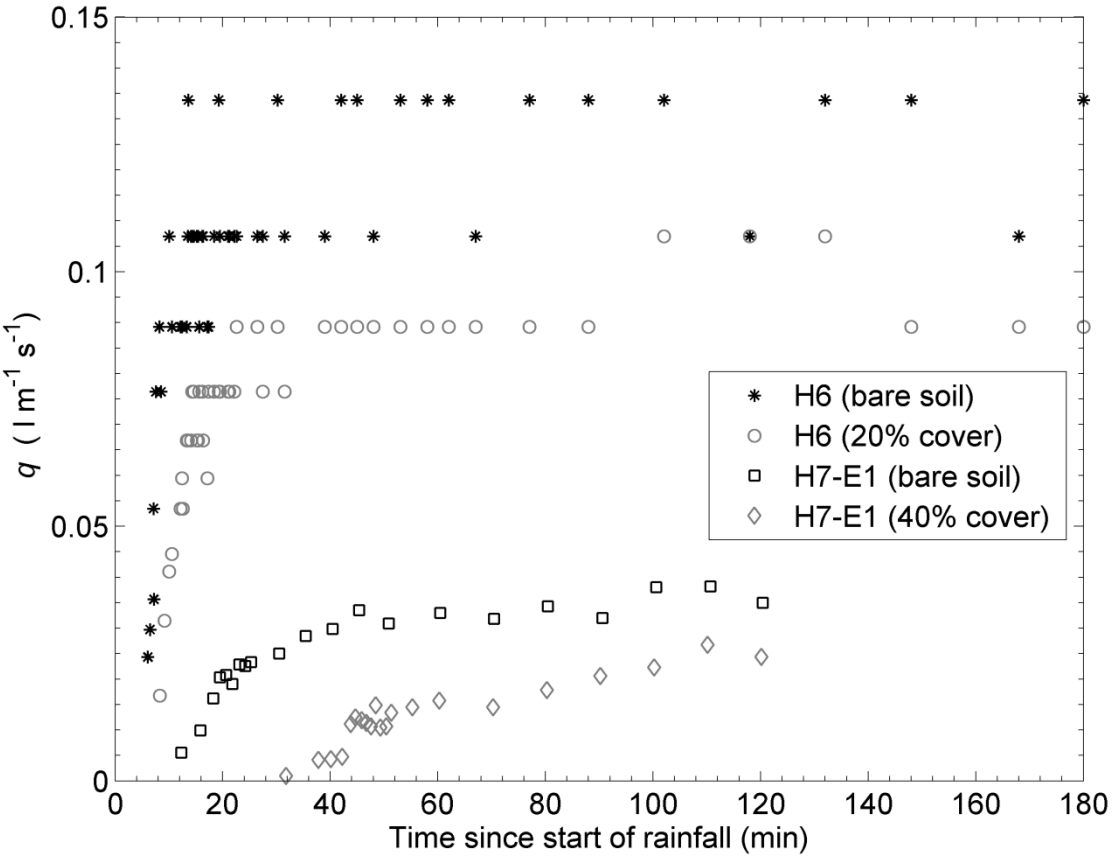

Figure 3. The measured discharges rates, *q*, of flumes 1 and 2 from start of rainfall for experiments H6 and H7-H1. The presence of rock fragments on the topsoil retards the runoff generation and reduces the steady-state discharge rate during both experiments. The overall effect of the rock fragments varies with rainfall rate and the rock fragment coverage. The measured discharge rate from flume 2 during H7-E1 shows that 2 h was insufficient to reach the steady-state discharge using low rainfall intensity (28 mm h^{-1}) and high rock fragment cover (40%).

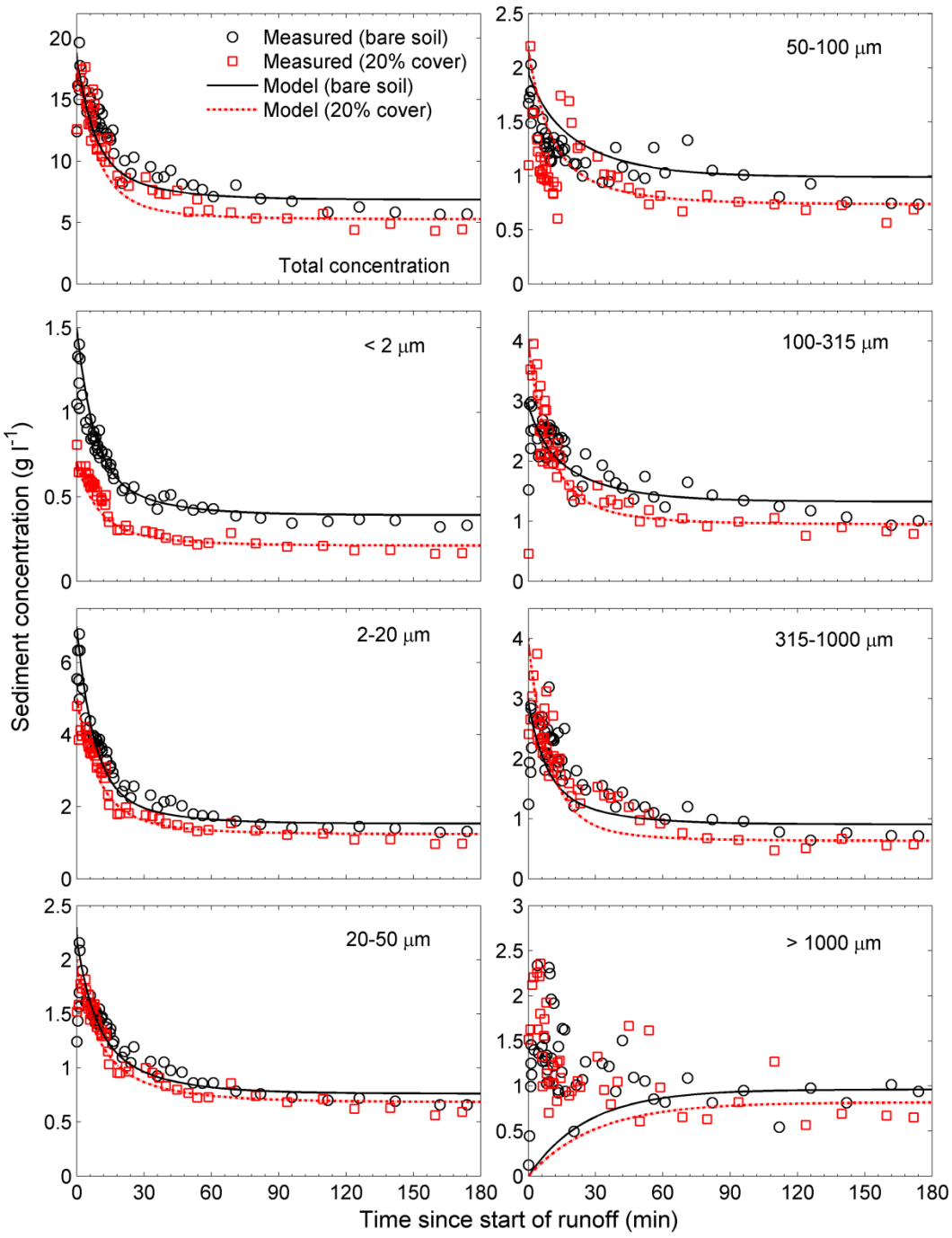

Figure 4. Measured data and numerical modeling results for experiment H6. Model parameters were initially fit to experimental data collected in flume 1 (without rock fragments) using the results of *Jomaa et al.* [2010] as initial guesses. The optimized parameters were then used to model the data collected on flume 2 (20% rock fragment cover).

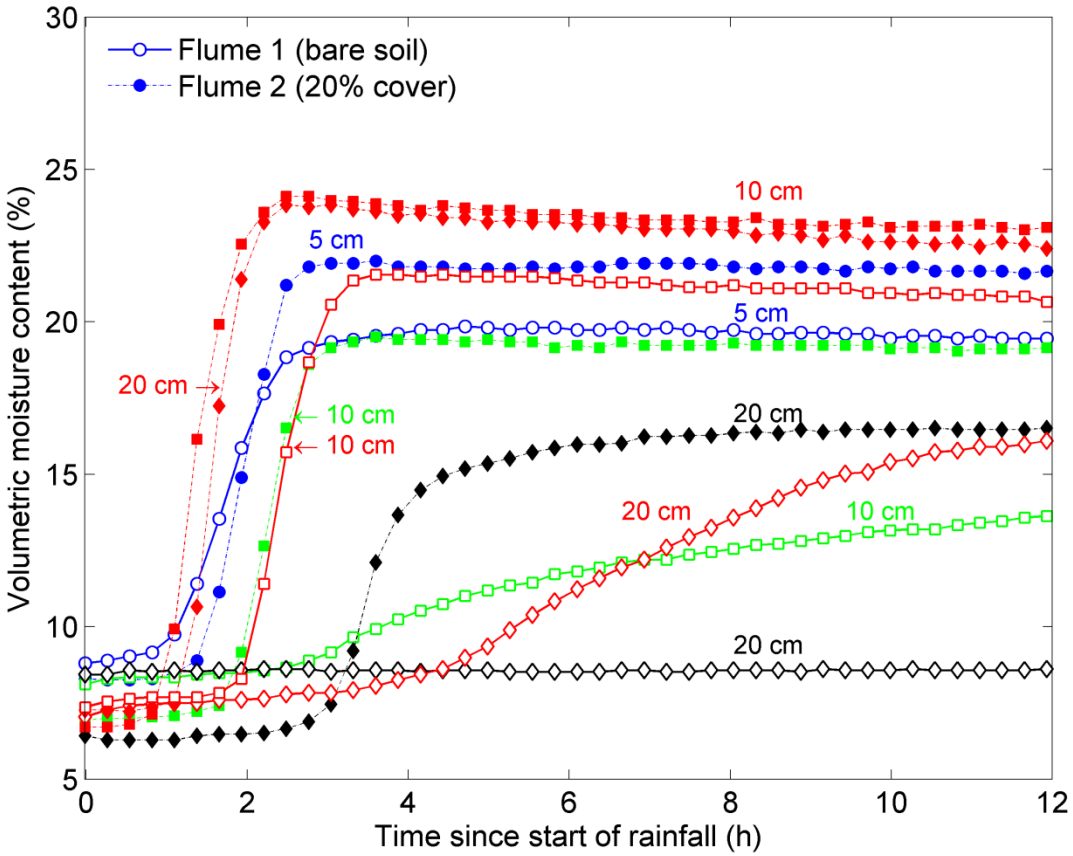

Figure 5. The measured volumetric moisture content for experiment H6 at different soil depths and flume locations (see also Figure 1). The open and filled markers distinguish between flume 1 and 2. Different color and line markers (blue circle, green square, black diamond) correspond to different measurement depths in the soil profile (5, 10 and 20 cm, respectively). These measurements correspond to locations that received more uniform precipitation. However, the red curves correspond to a locations (10 and 20 cm) affected by overlapping sprinklers (Figure 2). Results suggest that rock fragment coverage increases moisture content and the rate of moisture penetration into the soil compared with bare soil. The effect of overlapping sprinklers was to increase the moisture content in both flumes, but the moisture increase was more marked for the bare soil.

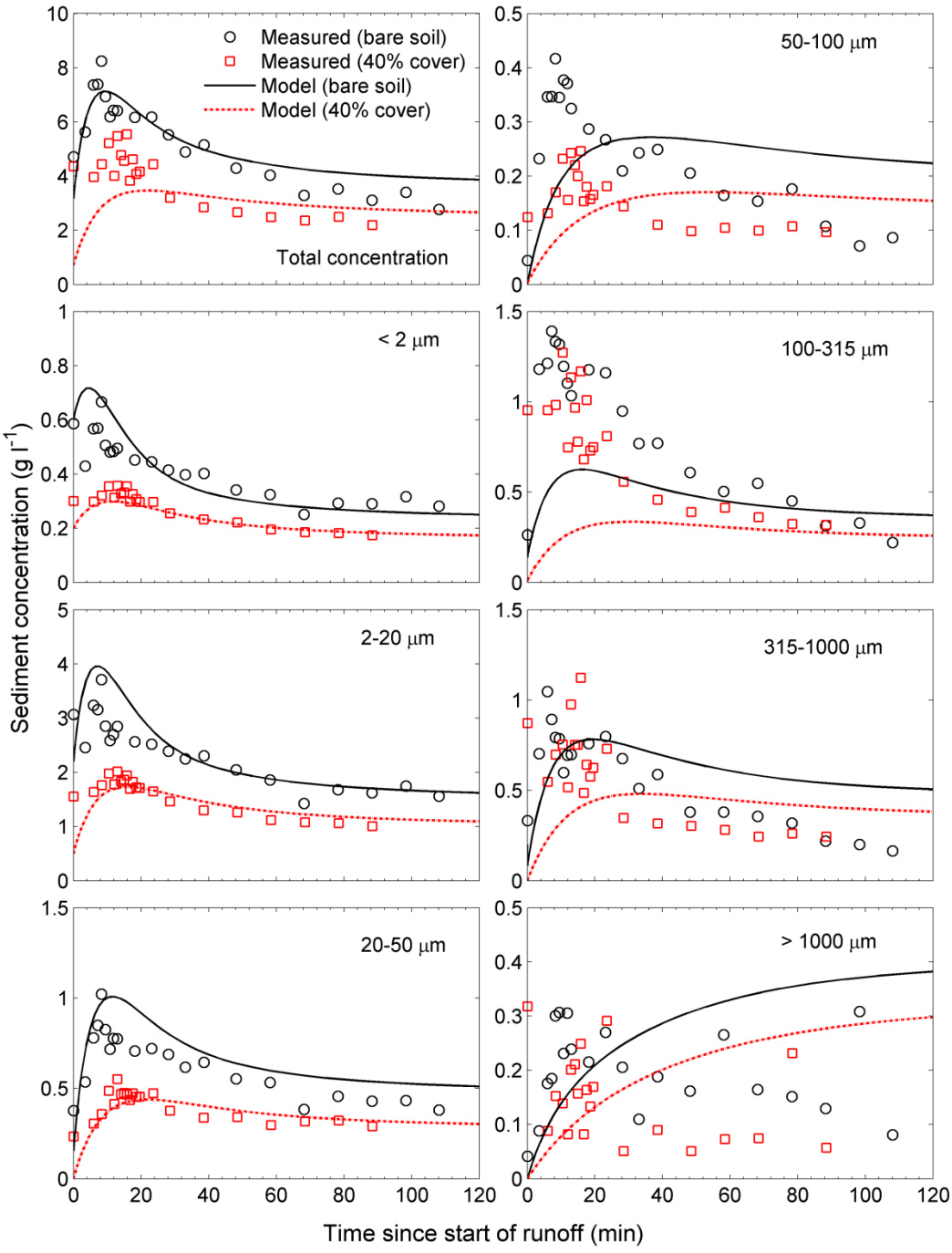

Figure 6. Observed and fitted concentrations for experiment H7-E1 using the H-R model. The model reproduced reasonably the total and the finer size classes sediment concentrations. However, it could not predict the mid- and larger size classes. The results (concentrations still varying at the end of the experiment) show that the steady-state behavior required more than 2 h to be reached.

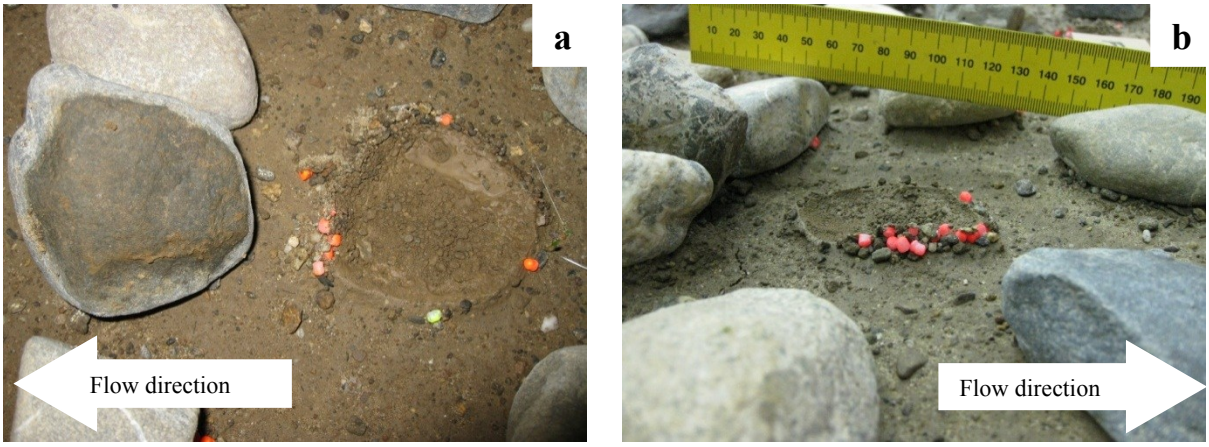

Figure 7. Pictures taken after the H6 erosion event showing the local effect of the rock fragments. Panels a and b show soil underneath two different rock fragments. Both pictures illustrate that, under the rock fragment, the soil retains its initial state (unsealed) – increasing the infiltration rate – with material trapped around the rock fragment's edge. The moisture content beneath the rock fragment increased significantly, however. The area between the rock fragments was compacted by raindrops. The image also shows neutrally buoyant colored plastic particles (released in a transverse line at about 0.5 m in Figure 2) that were used to provide an independent (of the original soil) qualitative measure of particle trapping by rock fragments. Colored particles were mainly trapped under the downslope edge of the rock fragments.

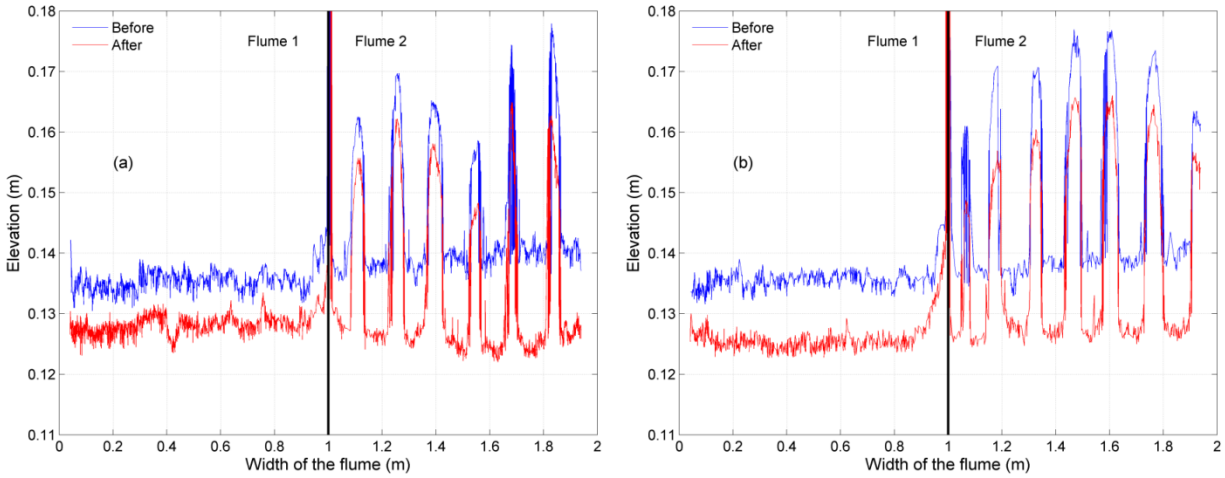

Figure 8. Soil surface elevation along the two transects shown in Figure 1, before (blue line) and after (red) experiment H6. Panel a (transect at 1.8m), is representative of changes occurring where soil is affected by uniform precipitation, while panel b (transect at 2.5m) corresponds to a location with overlapping sprinklers. With uniform precipitation, soil compaction and surface sealing varies between 6-8 mm for the bare soil to 8-15 mm with rock fragment coverage. In the overlapping areas, the flumes show a similar elevation change, possibly due to the increase in moisture content and raindrop compaction. Panels a and b (in flume 2) illustrate that soil under rock fragments is also compacted. Clearly, the compaction under the rock fragments (where surface sealing did not occur) is lower than the rest of the transversal line (panel a) reflecting the effect of surface sealing on soil elevation.